J|A|C|S ARTICLES

Published on Web 12/15/2009

Guest-Encapsulation Properties of a Self-Assembled Capsule by Dynamic Boronic Ester Bonds

Naoki Nishimura,[†] Kenji Yoza,[‡] and Kenji Kobayashi*[,†]

Department of Chemistry, Faculty of Science, Shizuoka University, 836 Ohya, Suruga-ku, Shizuoka 422-8529, Japan, and Bruker AXS, 3-9-B Moriya, Kanagawa-ku, Yokohama 221-0022, Japan

Received October 6, 2009; E-mail: skkobay@ipc.shizuoka.ac.jp

Abstract: Two molecules of tetrakis(dihydroxyboryl)-cavitand **1a** as an aromatic cavity and four molecules of 1,2-bis(3,4-dihydroxyphenyl)ethane **2** as an equatorial linker self-assemble into capsule **3a** via the formation of eight dynamic boronic ester bonds in $CDCl_3$ or C_6D_6. Capsule **3a** encapsulates one guest molecule, such as 4,4′-disubstituted-biphenyl and 2,6-disubstituted-anthracene derivatives, in a highly selective recognition event, wherein the guest substituents are oriented to both aromatic cavity ends of **3a**, as confirmed by a ^{1}H NMR study and X-ray crystallographic analysis. Capsule **3a** showed a significant solvent effect on guest encapsulation. The association constant (K_a) of **3a** with guests in C_6D_6 was much greater than that in $CDCl_3$ (450−48 000-fold). The encapsulation of guests within **3a** in C_6D_6 was enthalpically driven, whereas that in $CDCl_3$ tended to be both enthalpically and entropically driven. Thermodynamic studies suggest that the small K_a value in $CDCl_3$ arises from the character of $CDCl_3$ as a competitor guest molecule for **3a**, and not from the difference in stability of the boronic ester bonds of **3a** in both solvents. We propose a linker partial dissociation mechanism for the guest uptake and release into and out of **3a** based on the kinetic studies of guest@**3a** using 2D EXSY analysis, as well as structural analysis of a guest@**3b**. The rotation behavior of 4,4′-diacetoxy-2,2′-disubstituted-biphenyls within **3a** was also investigated, where the elongation of 2,2′-disubstituents of guests put the brakes on guest rotation within **3a**.

Introduction

Carcerands and hemicarcerands, in which two calix[4]resorcinarene cavitands are held together by four covalent linkages, have been developed by Cram and others and have attracted considerable attention from the viewpoint of stabilization of reactive intermediates and as microvesicles for drug delivery, given the confinement of guest molecules inside the capsules away from a bulk phase.[1] Error correction through thermodynamic equilibration, minimization of synthetic effort by use of modular subunits, and control of assembly processes through subunit design are characteristics of supramolecular approaches to self-assembly. Based on this concept, cavitand-based capsules have been constructed under thermodynamic control using noncovalent interactions, such as hydrogen bonds,[2] metal-coordination bonds,[3] ionic interactions,[4] and solvophobic interactions.[5] As an alternative strategy, dynamic covalent chemistry offers great advantages in supramolecular syntheses because dynamic covalent bonds contain reversible covalent bond-forming and bond-breaking processes under thermodynamic control; namely, they combine both the strength of covalent bonds and the reversibility of noncovalent interactions.[6] The reversibility of the imine bond-forming reaction in the presence of a catalytic amount of CF_3CO_2H has been applied to cavitand-based capsule synthesis.[7] The use of a redox buffer has allowed a disulfide-linked cavitand capsule to form under reversible conditions.[8] Boronic ester formation is another reliable synthon for dynamic covalent chemistry.[9] Supramolecular syntheses based on the reversible formation of boronic or boronate esters, such as polymers,[10] macrocycles,[11] and capsules,[12] have been reported recently. Self-assembled architectures using spiroborate formation have also been synthesized.[13] However, the supramolecular synthesis of cavitand-based capsules via the dynamic formation of boronic esters has not been achieved so far. Recently, we have reported the self-

[†] Shizuoka University.
[‡] Bruker AXS.

(1) (a) Cram, D. J.; Cram, J. M. *Container Molecules and Their Guests*; Royal Society of Chemistry: Cambridge, 1994. (b) Jasat, A.; Sherman, J. C. *Chem. Rev.* **1999**, *99*, 931–967. (c) Warmuth, R.; Yoon, J. *Acc. Chem. Res.* **2001**, *34*, 95–105. (d) Sherman, J. *Chem. Commun.* **2003**, 1617–1623. (e) Barrett, E. S.; Irwin, J. L.; Edward, A. J.; Sherburn, M. S. *J. Am. Chem. Soc.* **2004**, *126*, 16747–16749. (f) Makeiff, D. A.; Sherman, J. C. *J. Am. Chem. Soc.* **2005**, *127*, 12363–12367. (g) Warmuth, R.; Makowiec, S. *J. Am. Chem. Soc.* **2007**, *129*, 1233–1241.

(2) (a) Chapman, R. G.; Sherman, J. C. *J. Am. Chem. Soc.* **1995**, *117*, 9081–9082. (b) MacGillivray, L. R.; Atwood, J. L. *Nature* **1997**, *389*, 469–472. (c) Heinz, T.; Rudkevich, D. M.; Rebek, J., Jr. *Nature* **1998**, *394*, 764–766. (d) Shivanyuk, A.; Paulus, E. F.; Böhmer, V. *Angew. Chem., Int. Ed.* **1999**, *38*, 2906–2909. (e) Kobayashi, K.; Shirasaka, T.; Yamaguchi, K.; Sakamoto, S.; Horn, E.; Furukawa, N. *Chem. Commun.* **2000**, 41–42. (f) Ebbing, M. H. K.; Villa, M.-J.; Valpuesta, J.-M.; Prados, P.; de Mendoza, J. *Proc. Natl. Acad. Sci. U.S.A.* **2002**, *99*, 4962–4966. (g) Kobayashi, K.; Ishii, K.; Sakamoto, S.; Shirasaka, T.; Yamaguchi, K. *J. Am. Chem. Soc.* **2003**, *125*, 10615–10624. (h) Sansone, F.; Baldini, L.; Casnati, A.; Chierici, E.; Faimani, G.; Ugozzoli, F.; Ungaro, R. *J. Am. Chem. Soc.* **2004**, *126*, 6204–6205. (i) Ajami, D.; Rebek, J., Jr. *J. Am. Chem. Soc.* **2006**, *128*, 5314–5315. (j) Yamanaka, M.; Ishii, K.; Yamada, Y.; Kobayashi, K. *J. Org. Chem.* **2006**, *71*, 8800–8806. (k) Kitagawa, H.; Kobori, Y.; Yamanaka, M.; Yoza, K.; Kobayashi, K. *Proc. Natl. Acad. Sci. U.S.A.* **2009**, *106*, 10444–10448.

assembly of tetrakis(dihydroxyboryl)-cavitand **1a** as a polar bowl-shaped aromatic cavity and 1,2-bis(3,4-dihydroxyphenyl)ethane **2** as an equatorial bis(catechol)-linker[14] into capsule

Scheme 1. Formation of Capsule **3** from Cavitand Tetraboronic Acid **1** and Bis(catechol)-Linker **2**[a]

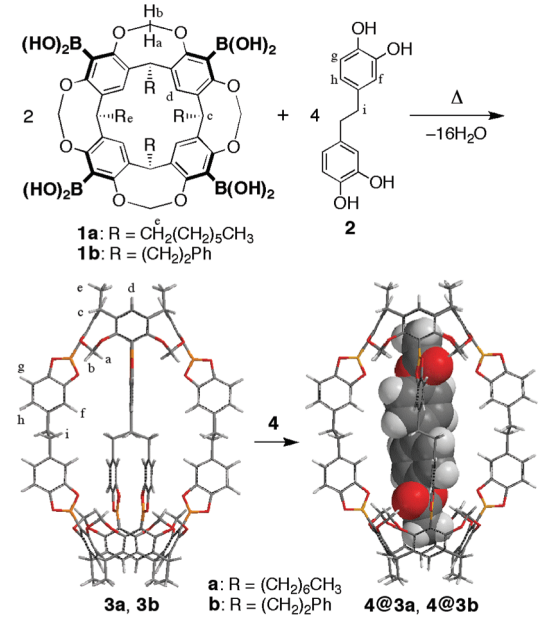

[a] Molecular models of **3** and 4,4′-diacetoxybiphenyl encapsulating capsule **4@3** are calculated at the PM3 level of Spartan ′06,[20] wherein the side chains R of **3** are replaced by methyl groups.

3a via the dynamic formation of boronic esters (Scheme 1).[15] The self-assembled cavitand-based capsule **3a** encapsulates one guest molecule, such as 4,4′-disubstituted-biphenyl. The merit of **3a** based on the dynamic boronic ester bond is the on/off control of capsule formation with guest encapsulation by the removal/addition of MeOH.[15] Herein, we report on a comprehensive study on the guest-encapsulation properties of the self-assembled capsule **3a**, including X-ray crystal structure, guest-encapsulation selectivity, remarkable solvent effect on guest encapsulation, and thermodynamics and kinetics on guest encapsulation. We propose a linker partial dissociation mechanism for guest encapsulation and release into and out of **3a**. We also describe guest-rotation behavior within **3a** directed toward the formation of a supramolecular gyroscope.

Results and Discussion

Synthesis of Self-Assembled Cavitand-Based Capsule 3a: ^{1}H NMR Study. The cavitand tetraboronic acid **1a** (side chain, R = $(CH_2)_6CH_3$)[15,16] and the bis(catechol)-linker **2**[15] have low solubility in $CDCl_3$ by themselves. However, a 2:4 heterogeneous mixture of **1a** and **2** in $CDCl_3$ gives a homogeneous solution on heating at 323 K for 3 h, and this quantitatively produces capsule **3a** (Scheme 1).[15] The ^{1}H NMR spectrum of the reaction mixture shows a highly symmetrical single species and the disappearance of the OH groups of the **1a** and **2** units (Figure 1c vs Figure 1a and 1b), indicating the quantitative formation of **3a**. The ^{1}H NMR chemical shift change of **3a** relative to **1a** and **2**, $\Delta\delta$ ($\delta_{complex} - \delta_{free}$), is 0.14, −0.20, 0.10,

(3) (a) Jacopozzi, P.; Dalcanale, E. *Angew. Chem., Int. Ed. Engl.* **1997**, *36*, 613–615. (b) Fox, O. D.; Dalley, N. K.; Harrison, R. G. *J. Am. Chem. Soc.* **1998**, *120*, 7111–7112. (c) Ikeda, A.; Yoshimura, M.; Udzu, H.; Fukuhara, C.; Shinkai, S. *J. Am. Chem. Soc.* **1999**, *121*, 4296–4297. (d) Fox, O. D.; Drew, M. G. B.; Beer, P. D. *Angew. Chem., Int. Ed.* **2000**, *39*, 136–140. (e) Pinalli, R.; Cristini, V.; Sottili, V.; Geremia, S.; Campagnolo, M.; Caneschi, A.; Dalcanale, E. *J. Am. Chem. Soc.* **2004**, *126*, 6516–6517. (f) Kobayashi, K.; Yamada, Y.; Yamanaka, M.; Sei, Y.; Yamaguchi, K. *J. Am. Chem. Soc.* **2004**, *126*, 13896–13897. (g) Haino, T.; Kobayashi, M.; Chikaraishi, M.; Fukazawa, Y. *Chem. Commun.* **2005**, 2321–2323. (h) Park, S. J.; Shin, D. M.; Sakamoto, S.; Yamaguchi, K.; Chung, Y. K.; Lah, M. S.; Hong, J.-I. *Chem.—Eur. J.* **2005**, *11*, 235–241. (i) Jude, H.; Sinclair, D. J.; Das, N.; Sherburn, M. S.; Stang, P. J. *J. Org. Chem.* **2006**, *71*, 4155–4163.
(4) (a) Corbellini, F.; Fiammengo, R.; Timmerman, P.; Crego-Calama, M.; Versluis, K.; Heck, A. J. R.; Luyten, I.; Reinhoudt, D. N. *J. Am. Chem. Soc.* **2002**, *124*, 6569–6575. (b) Oshovsky, G. V.; Reinhoudt, D. N.; Verboom, W. *J. Am. Chem. Soc.* **2006**, *128*, 5270–5278.
(5) (a) Gibb, C. L.; Gibb, B. C. *J. Am. Chem. Soc.* **2004**, *126*, 11408–11409. (b) Giles, M. D.; Liu, S.; Emanuel, R. L.; Gibb, B. C.; Grayson, S. M. *J. Am. Chem. Soc.* **2008**, *130*, 14430–14431.
(6) (a) Lehn, J.-M. *Chem.—Eur. J.* **1999**, *5*, 2455–2463. (b) Rowan, S. J.; Cantrill, S. J.; Cousins, G. R. L.; Sanders, J. K. M.; Stoddart, J. F. *Angew. Chem., Int. Ed.* **2002**, *41*, 898–952. (c) Severin, K. *Chem.—Eur. J.* **2004**, *10*, 2565–2580. (d) Corbett, P. T.; Leclaire, J.; Vial, L.; West, K. R.; Wietor, J.-L.; Sanders, J. K. M.; Otto, S. *Chem. Rev.* **2006**, *106*, 3652–3711. (e) Mal, P.; Schultz, D.; Beyer, K.; Rissanen, K.; Nitschke, J. R. *Angew. Chem., Int. Ed.* **2008**, *47*, 8297–8301.
(7) (a) Ro, S.; Rowan, S. J.; Pease, A. R.; Cram, D. J.; Stoddart, J. F. *Org. Lett.* **2000**, *2*, 2411–2414. (b) Liu, X.; Liu, Y.; Li, G.; Warmuth, R. *Angew. Chem., Int. Ed.* **2006**, *45*, 901–904. (c) Liu, X.; Warmuth, R. *J. Am. Chem. Soc.* **2006**, *128*, 14120–14127. (d) Liu, Y.; Liu, X.; Warmuth, R. *Chem.—Eur. J.* **2007**, *13*, 8953–8959. (e) Xu, D.; Warmuth, R. *J. Am. Chem. Soc.* **2008**, *130*, 7520–7521. (f) Skowronek, P.; Gawronski, J. *Org. Lett.* **2008**, *10*, 4755–4758.
(8) Sun, J.; Patrick, B. O.; Sherman, J. C. *Tetrahedron* **2009**, *65*, 7296–7302.
(9) (a) Fujita, N.; Shinkai, S.; James, T. D. *Chem. Asian J.* **2008**, *3*, 1076–1091. (b) Zhu, L.; Shabbir, S. H.; Gray, M.; Lynch, V. M.; Sorey, S.; Anslyn, E. V. *J. Am. Chem. Soc.* **2006**, *128*, 1222–1232.
(10) For self-assembled polymers based on boronic ester formation, see: (a) Côté, A. P.; Benin, A. I.; Ockwig, N. W.; O'Keeffe, M.; Matzger, A. J.; Yaghi, O. M. *Science* **2005**, *310*, 1166–1170. (b) Niu, W.; O'Sullivan, C.; Rambo, B. M.; Smith, M. D.; Lavigne, J. J. *Chem. Commun.* **2005**, 4342–4344. (c) Tilford, R. W.; Gemmill, W. R.; zur Loye, H.-C.; Lavigne, J. J. *Chem. Mater.* **2006**, *18*, 5296–5301. (d) Niu, W.; Smith, M. D.; Lavigne, J. J. *J. Am. Chem. Soc.* **2006**, *128*, 16466–16467. (e) El-Kaderi, H. M.; Hunt, J. R.; Mendoza-Cortés, J. L.; Côté, A. P.; Taylor, R. E.; O'Keeffe, M.; Yaghi, O. M. *Science* **2007**, *316*, 268–272. (f) Côté, A. P.; El-Kaderi, H. M.; Furukawa, H.; Hunt, J. R.; Yaghi, O. M. *J. Am. Chem. Soc.* **2007**, *129*, 12914–12915. (g) Tilford, R. W.; Mugavero, S. J.; Pellechia, P. J.; Lavigne, J. J. *Adv. Mater.* **2008**, *20*, 2741–2746. (h) Hunt, J. R.; Doonan, C. J.; LeVangie, J. D.; Côté, A. P.; Yaghi, O. M. *J. Am. Chem. Soc.* **2008**, *130*, 11872–11873.
(11) For self-assembled macrocycles based on boronic ester formation, see: (a) Christinat, N.; Scopelliti, R.; Severin, K. *Chem. Commun.* **2004**, 1158–1159. (b) Barba, V.; Villamil, R.; Luna, R.; Godoy-Alcántar, C.; Höpfl, H.; Beltram, H. I.; Zamudio-Rivera, L. S.; Santillan, R.; Farfán, N. *Inorg. Chem.* **2006**, *45*, 2553–2561. (c) Christinat, N.; Scopelliti, R.; Severin, K. *J. Org. Chem.* **2007**, *72*, 2192–2200. (d) Christinat, N.; Scopelliti, R.; Severin, K. *Angew. Chem., Int. Ed.* **2008**, *47*, 1848–1852. (e) Hutin, M.; Bernardinelli, G.; Nitschke, J. R. *Chem.—Eur. J.* **2008**, *14*, 4585–4593.
(12) For, self-assembled capsules based on boronic or boronate ester formation, see: (a) Iwasawa, N.; Takahagi, H. *J. Am. Chem. Soc.* **2007**, *129*, 7754–7755. (b) Kataoka, K.; James, T. D.; Kubo, Y. *J. Am. Chem. Soc.* **2007**, *129*, 15126–15127. (c) Içli, B.; Christinat, N.; Tönnemann, J.; Schüttler, C.; Scopelliti, R.; Severin, K. *J. Am. Chem. Soc.* **2009**, *131*, 3154–3155.
(13) For self-assemblies based on spiroborate, see: (a) Katagiri, H.; Miyagawa, T.; Furusho, Y.; Yashima, E. *Angew. Chem., Int. Ed.* **2006**, *45*, 1741–1744. (b) Danjo, H.; Hirata, K.; Yoshigai, S.; Azumaya, I.; Yamaguchi, K. *J. Am. Chem. Soc.* **2009**, *131*, 1638–1639.
(14) For catechol-based metal ion assisted self-assembly of capsules, see: (a) Schalley, C. A.; Lützen, A.; Albrecht, M. *Chem.—Eur. J.* **2004**, *10*, 1072–1080. (b) Fiedler, D.; Leung, D. H.; Bergman, R. G.; Raymond, K. N. *Acc. Chem. Res.* **2005**, *38*, 351–360.
(15) Nishimura, N.; Kobayashi, K. *Angew. Chem., Int. Ed.* **2008**, *47*, 6255–6258.
(16) Sherman, J. C.; Knobler, C. B.; Cram, D. J. *J. Am. Chem. Soc.* **1991**, *113*, 2194–2204.

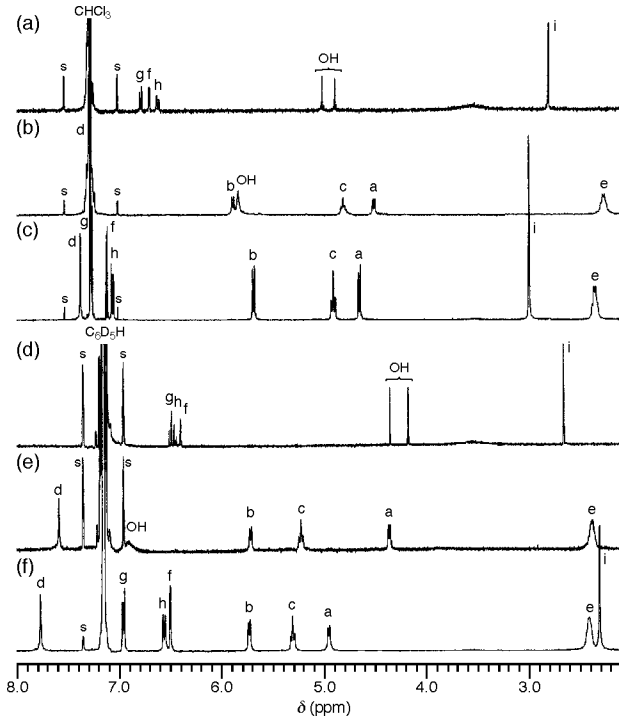

Figure 1. ^{1}H NMR spectra (400 MHz, 296 K). In $CDCl_3$, (a) [**2**] = 10 mM if soluble (heterogeneous), (b) [**1a**] = 5 mM if soluble, and (c) capsule **3a** (homogeneous after heating [**1a**] = 5 mM and [**2**] = 10 mM at 50 °C for 3 h. In C_6D_6, (d) [**2**] = 10 mM if soluble (heterogeneous), (e) [**1a**] = 5 mM if soluble, and (f) capsule **3a** (heterogeneous after heating [**1a**] = 5 mM and [**2**] = 10 mM at 50 °C for 3 h). The signals marked 'a−i' are assigned in Scheme 1. The signals marked 's' are the spinning sidebands of the residual solvent.

and 0.12 ppm for H_a-H_d of the **1a** unit, respectively, and 0.42, 0.49, 0.45, 0.20 ppm for H_f-H_i of the **2** unit, respectively.

Heating a 2:4 mixture of **1a** and **2** in C_6D_6 at 323 K for 3 h does not give a homogeneous system, although **3a** was formed quantitatively (Figure 1f). The solubility of **3a** in C_6D_6 at 296 K was 1.3 mM based on the ^{1}H NMR integration ratio with *p*-dimethoxybenzene as an internal standard. The $\Delta\delta$ values were 0.59, 0.02, 0.08, and 0.19 ppm for H_a-H_d of the **1a** unit, respectively, and 0.10, 0.46, 0.11, and −0.35 ppm for H_f-H_i of the **2** unit, respectively. In contrast, heating this mixture in the presence of an appropriate guest gives a homogeneous solution and quantitatively produces the guest-encapsulating capsule, guest@**3a** (vide infra).[15]

X-ray Crystal Structure of 4@3b. Single crystals of **4@3b** suitable for X-ray diffraction analysis were obtained by slow evaporation of a benzene solution of a 2:4:2 mixture of cavitand tetraboronic acid **1b** (side chain, R = $(CH_2)_2$Ph), bis(catechol)-linker **2**, and 4,4′-diacetoxybiphenyl **4** at room temperature after heating this mixture at 323 K for 3 h. The single-crystal X-ray diffraction measurement was performed at 100 K.[17] As shown in Figure 2a and 2b, two molecules of **1b** at the polar positions are indirectly held together by eight boronic ester bonds involving four molecules of **2** at the equatorial positions to self-assemble into capsule **3b**. Exactly one molecule of **4** is encapsulated in the cavity of **3b**, and the acetoxy groups at the 4,4′-positions of **4** are oriented toward the two aromatic cavity ends of **3b** to maximize the guest−capsule CH−π interaction.[18,19] This guest orientation is consistent with that determined previously by the ^{1}H NMR analysis of **4@3a** in solution.[15] The close C(=O)$CH_3\cdots C\pi$ contact distance between the acetoxy protons of **4** and the aromatic cavity of **3b** is ca. 2.80 Å. The carbonyl oxygen atoms of the acetoxy groups interact with inner protons of the methylene-bridge rims (O−C$H_{in}H_{out}$−O) of **3b** with C=O$\cdots H_{in}$C distances of 2.53 and 2.71 Å.[2k]

A molecular model of **3** (side chain of **1** unit, R = CH_3), calculated using the Spartan ′06 software package at the PM3 level,[20] suggests that four linker **2** units adopt an *anti*-conformation, and the northern polar **1** unit is twisted by ca. 12.4° with respect to the southern polar **1** unit about a C_4 polar axis (Scheme 1).[15] Namely, capsule **3** may exist as a 1:1 mixture of the twisted (*M*)- and (*P*)-enantiomers (twistomers),[21,22] when four linkers with *anti*-conformation are arranged in the same direction. However, this is not the case for the actual crystal structure of **4@3b**. All linker **2** units adopted an approximate *anti*-conformation, but they were highly disordered, even at 100 K, and were not necessarily arranged in the same direction (Figure 2c−2e).

In Figure 2c−2e, the occupancy factor (occ-f) of the B(1) atom was occ-f = 1.00, but the other three boron atoms were observed at two positions, wherein both the B(2) and B(3) atoms showed occ-f = 0.796 (orange colored atoms) and occ-f = 0.204 (blue colored atoms) and the B(4) atom showed occ-f = 0.50 each (orange and green colored atoms). The two linkers connecting the B(2) and B(3) atoms with the major occ-f, which are placed diagonally across from each other, are arranged in the opposite direction to produce a *meso*-form. The two linkers connecting the B(1) and B(4) atoms can be arranged in the same or opposite directions to give *enantio*- or *meso*-forms, respectively. Thus, the four linker **2** units in **3b** behave as semimobile linkers. As a result, in the crystal structure of **4@3b**, the northern and southern polar **1b** units were not twisted but were slipped ca. 0.8 Å relative to each other.[22b,23] In the crystal structure, **3b** exists as an average form of a mixture of the (*M*)- and (*P*)-twistomers and slipped-forms (Figure 2f) and possesses an inner cavity with an approximate dimension of 8.5 × 19.9 Å^2 (interatomic distances) and four equatorial portals with a dimension of approximately 6.7 × 11.9 Å^2. These dimensions are almost the same as those in the calculated twisted form of **3**.[15] Interconversion between the (*M*)- and (*P*)-twistomers and slipped forms in **3a** is very fast in solution, and their conformational isomers are observed as an average form.

IR Study of Guest@3a. The IR spectrum of **4@3a** (KBr) is characterized by the disappearance of the OH groups from **1a** and **2**, showing the formation of the boronic ester.[17] The C=O stretching band of the acetoxy group of **4@3a** appears at ν =

(17) See the Supporting Information.
(18) Kobayashi, K.; Ishii, K.; Yamanaka, M. *Chem.−Eur. J.* **2005**, *11*, 4725–4734.
(19) (a) Kobayashi, K.; Kitagawa, R.; Yamada, Y.; Yamanaka, M.; Suematsu, T.; Sei, Y.; Yamaguchi, K. *J. Org. Chem.* **2007**, *72*, 3242–3246. (b) Kitagawa, H.; Kawahata, M.; Kitagawa, R.; Yamada, Y.; Yamanaka, M.; Yamaguchi, K.; Kobayashi, K. *Tetrahedron* **2009**, *65*, 7234–7239.
(20) Spartan ′06; Wavefunction Inc.: Irvine, CA, USA, 2006.
(21) (a) Chapman, R. G.; Sherman, J. C. *J. Am. Chem. Soc.* **1999**, *121*, 1962–1963. (b) Paek, K.; Ihm, H.; Yun, S.; Lee, H. C. *Tetrahedron Lett.* **1999**, *40*, 8905–8909. (c) Chapman, R. G.; Sherman, J. C. *J. Org. Chem.* **2000**, *65*, 513–516.
(22) (a) Cram, D. J.; Blanda, M. T.; Paek, K.; Knobler, C. B. *J. Am. Chem. Soc.* **1992**, *114*, 7765–7773. (b) Robbins, T. A.; Knobler, C. B.; Bellew, D. R.; Cram, D. J. *J. Am. Chem. Soc.* **1994**, *116*, 111–122.
(23) (a) v. d. Bussche-Hünnefeld, C.; Bühring, D.; Knobler, C. B.; Cram, D. J. *J. Chem. Soc., Chem. Commun.* **1995**, *108*, 5–1087. (b) Helgeson, R. C.; Paek, K.; Knobler, C. B.; Maverick, E. F.; Cram, D. J. *J. Am. Chem. Soc.* **1996**, *118*, 5590–5604. (c) Helgeson, R. C.; Knobler, C. B.; Cram, D. J. *J. Am. Chem. Soc.* **1997**, *119*, 3229–3244.

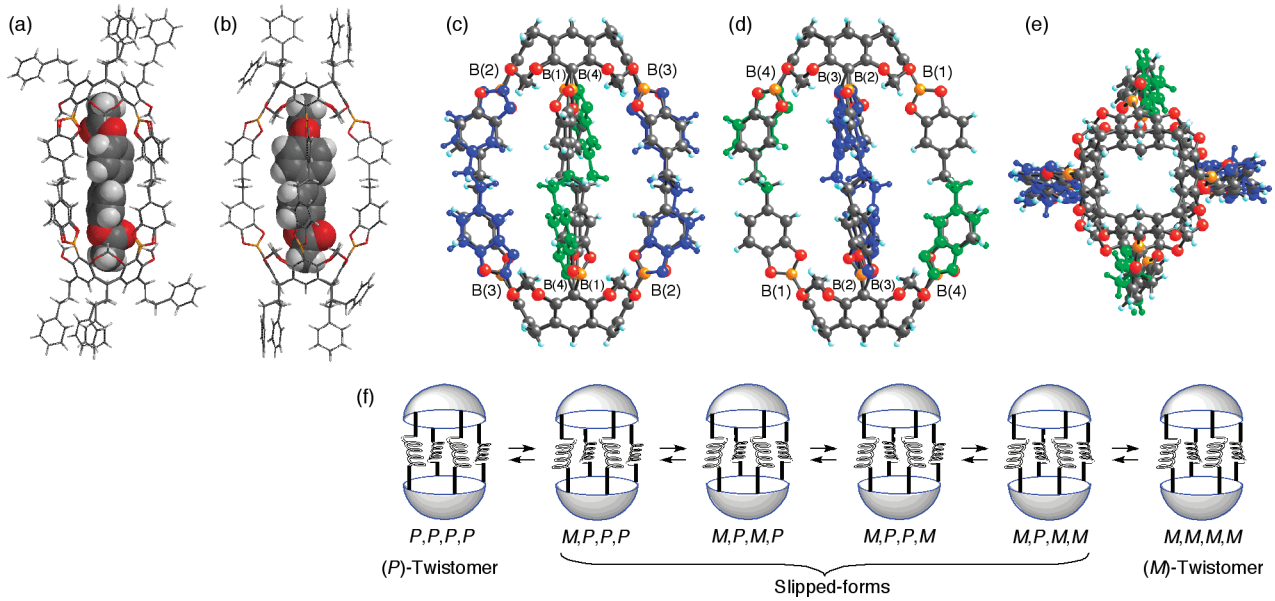

Figure 2. X-ray crystal structure of **4@3b** at 100 K. One of molecular structures of **4@3b**: (a) front view and (b) its 45°-rotation view, wherein two linkers with occupancy factor (occ-f) of 0.796 are placed at the diagonal position and two linkers (one side) with occ-f of 0.500 are placed at the other diagonal position. Molecular structures of **3b** containing all disordered linkers: (c) front view, (d) side view, and (e) top view, wherein the linkers with B(2) and B(3) are shown in gray (occ-f = 0.796) and blue (occ-f = 0.204) and the half-linkers with B(4) are shown in gray and green (occ-f = 0.50 each). (f) Schematic representation of conformational isomers of **3b**. In Figure 2c−f, the side chains of **3b** and encapsulated **4** are omitted for clarity.

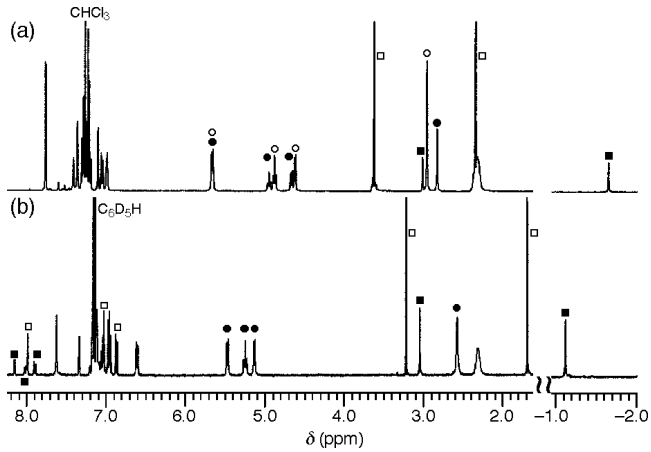

Figure 3. Association behavior of capsule **3a** with guest **8** monitored by ^{1}H NMR (400 MHz): (a) [**3a**] = 2.5 mM and [**8**] = 12.5 mM in $CDCl_3$ at 298 K and (b) [**3a**] = 0.5 mM and [**8**] = 1.0 mM in C_6D_6 at 313 K. The solid circle, open circle, solid square, and open square indicate the representative signals of **3a** of **8@3a**, free **3a**, **8** of **8@3a**, and free **8**, respectively.

1761 cm^{-1}, which is shifted to a higher wavenumber by 16 cm^{-1} relative to the spectrum of **4** alone. In **11@3a**, where **11** is 2,6-diacetoxy-9,10-anthraquinone, the C═O stretching bands of the acetoxy group and quinone moiety are shifted to higher wavenumbers by 13 and 4 cm^{-1}, respectively, relative to the spectrum of **11** alone.[17] These results suggest that the acetoxy groups are constricted by both aromatic cavity ends of **3a**.

^{1}H NMR Study of Guest@3a: Guest-Encapsulation Selectivity and Solvent Effect. A ^{1}H NMR study for the encapsulation of **4** in **3a** has been reported previously.[15] Figure 3 shows the ^{1}H NMR spectra for the encapsulation of 4,4′-diacetoxy-2,2′-bis(methoxycarbonyl)biphenyl **8** within **3a**. When 5 equiv of **8** was added to **3a** (2.5 mM) in $CDCl_3$, three species were independently observed after heating (Figure 3a), i.e., 34% guest-encapsulating capsule **8@3a**, 66% guest-free **3a**, and excess **8**. This result indicates that the exchange of **8** into and out of **3a** is slow on the NMR time scale. The ^{1}H NMR signals of **8** encapsulated in **3a** were shifted upfield by 3.99 ppm for the acetoxy protons and 0.61 ppm for the methyl ester protons relative to those of free **8**; namely, in **8@3a** the acetoxy protons are shifted much more upfield than the methyl ester protons are. This result clearly shows that the acetoxy groups at the 4,4′-positions are oriented toward both polar aromatic cavity ends of **3a** and the methyl ester groups at the 2,2′-positions are directed toward the equatorial portals of **3a** (Figure 4). This guest orientation in solution is in good agreement with that shown in the X-ray crystal structure of **4@3b**. Based on the integration ratio of the ^{1}H NMR signals, capsule **3a** encapsulates one molecule of **8**, and the association constant (K_a) of **3a** with **8** was estimated to be K_a = 44 M^{-1} in $CDCl_3$ at 298 K.

Heating a 2:4:2 mixture of **1a**, **2**, and **8** or a 1:2 mixture of as-prepared **3a** and **8** ([**8**] = 1 mM) in C_6D_6 at 323 K for 3 h gave a 1:1 mixture of **8@3a** and **8** (Figure 3b), wherein the guest exchange was slow on the NMR time scale. No guest-free **3a** was observed, indicating a very large value of K_a in C_6D_6 compared with the value of K_a in $CDCl_3$. The ^{1}H NMR signals of **8@3a** in C_6D_6 were shifted upfield by 2.81 ppm for the acetoxy protons and 0.17 ppm for the methyl ester protons relative to those of free **8**. The relatively smaller change in

(24) The ^{1}H NMR chemical shifts (δ) of the acetoxy and methyl ester protons of free **8** and **8@3a** were as follows: for free **8**, 2.33 (acetoxy) and 3.63 ppm (methyl ester) in $CDCl_3$ and 1.70 and 3.22 ppm in C_6D_6; for **8@3a**, −1.66 and 3.02 ppm in $CDCl_3$ and −1.11 and 3.05 ppm in C_6D_6. Thus, $\Delta\delta_G$ ($\delta_{encapsulated\text{-}guest} - \delta_{free\text{-}guest}$) values of **8** in C_6D_6 showed less upfield shifts by ca. 0.4−1.2 ppm relative to those in $CDCl_3$. This result can be interpreted as follows. (1) Free **8** is solvated by C_6D_6 and is subject to the ring current effect of C_6D_6-solvation. (2) Upon encapsulation of **8** in **3a**, desolvation of C_6D_6 from **8** occurs, and the **8** encapsulated in **3a** is no longer subject to the ring current effect of C_6D_6-solvation. (3) Instead, the **8** encapsulated in **3a** is subject to the ring current effect of the aromatic cavity of **3a**. Consequently, the $\Delta\delta_G$ values of **8** in C_6D_6 are cancelled and seemingly shifted less upfield relative to those in $CDCl_3$.

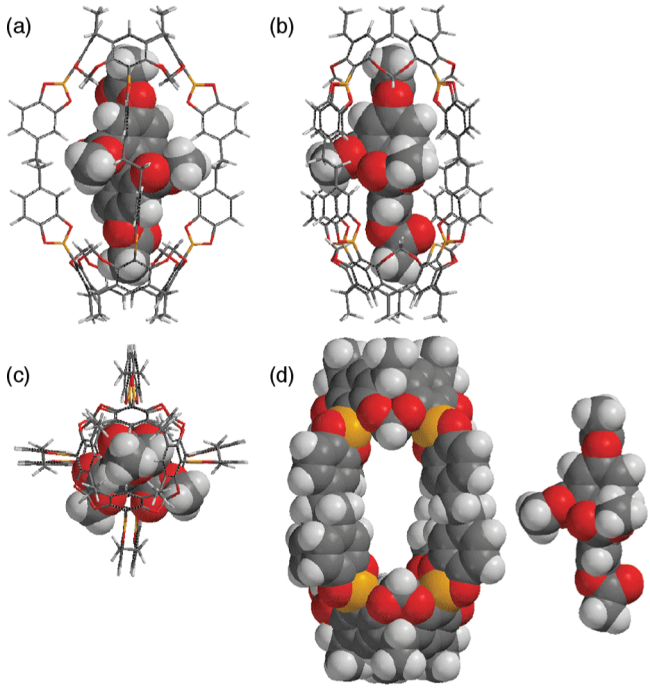

Figure 4. Molecular model of **8**@**3** calculated with Spartan ′06 at the PM3 level:[20] (a) front, (b) 45°-rotation, and (c) top views. (d) Space-filling representations of guest-free **3** and **8**. The side chains of **3** are replaced by methyl groups.

chemical shift in C_6D_6 than that in $CDCl_3$ upon encapsulation of **8** in **3a** is the result of a solvent effect.[24]

Guest molecules **4**−**20** encapsulated in **3a** are shown in Chart 1. In all cases, except for **20**, the exchange of guests into and out of **3a** was slow on the NMR time scale in both $CDCl_3$ and C_6D_6, as shown in Figure 3 for **8**@**3a**.[17] Thus, using the ^{1}H NMR integration change in signal of guest@**3a** as a function of the guest concentration, the association constant (K_a) of **3a** with guests can be estimated.[25] When the value of K_a is very large, a comparison of the signal integration between guest@**3a** and standard-guest@**3a**, namely, competitive encapsulation experiments, can be used to evaluate the guest-encapsulation ability of **3a**.[17] In all cases, guest exchanges between guest-A@**3a** and guest-B were fast on the human time scale and reached equilibration within a period of 5−10 min in both $CDCl_3$ and C_6D_6 at room temperature, but these are very slow on the NMR time scale, and the ^{1}H NMR signals of guest@**3a** and standard-guest@**3a** were independently observed. Thus, before the measurements of K_a, a mixture of as-prepared **3a**, guest-A, and guest-B (standard-guest) in $CDCl_3$ and C_6D_6 was heated at 323 K for 1 h in competitive encapsulation experiments. The value of K_a of **3a** with guests in $CDCl_3$ at 298 K and in C_6D_6 at 313 K and the change in ^{1}H NMR chemical shift of guest@**3a** relative to the free guests at the terminal functional groups ($\Delta\delta_G = \delta_{encapsulated\text{-}guest} - \delta_{free\text{-}guest}$) are summarized in Table 1. For comparison, the previously reported data for **4**, **5**, **6**, and **12** are also shown in Table 1.[15] The following features (Items 1−5) are noteworthy concerning the guest encapsulation in **3a**.

(25) The exchange of **20** in and out of **3a** was fast on the NMR time scale in C_6D_6, and the signals were observed as averaged forms. Thus, the K_a of **3a** with **20** in C_6D_6 at 313 K was calculated from a nonlinear curve fitting, wherein [**3a**] = 2.5 mM (constant) and [**20**] = 2.0−10.0 mM (variable).

Item 1. The values of $\Delta\delta_G$ of **5**−**7**, **9**−**14**, and **17**−**19** were almost the same as those of **4** and **8**, mentioned above. This result shows that all guests encapsulated in **3a** are oriented with the guest long axis aligned along the long axis of capsule **3a**.

Item 2. The value of K_a of guest@**3a** in C_6D_6 increases in the order **20** < **16** < **18** < **17** < **19** < **14** < **15** < **6** < **7** < **5** < **13** < **10** < **9** < **8** < **4** < **12** < **11**, whereas the value of K_a of guest@**3a** in $CDCl_3$ increases in the order **6** < **10** < **13** ≤ **15** < **9** < **5** < **12** < **8** < **7** < **4** < **11**. In $CDCl_3$, encapsulation of **14** and **16**−**20** was scarcely detected. Although the guest-binding order of **3a** in C_6D_6 is not necessarily consistent with that in $CDCl_3$, it is noteworthy that the value of K_a of guest@**3a** in C_6D_6 is 2 to 4 orders of magnitude greater than the value of K_a of guest@**3a** in $CDCl_3$ (K_a(in C_6D_6)/K_a(in $CDCl_3$) = 450−(4.8×10^4)). Thus, **3a** shows a significant solvent effect on guest encapsulation.

Item 3. Capsule **3a** strictly discriminates between functional groups of a guest. In a series of 4,4′-disubstituted-biphenyl derivatives with a similar molecular length, the value of K_a of guest@**3a** in C_6D_6 increases in the order **17** (4,4′-C(=O)OCH_3, K_a = 567 M^{-1}) ≪ **6** (4,4′-OCH_2CH_3, $K_a = 1.30 \times 10^4$ M^{-1}) < **5** (4-OC(=O)CH_3-4′-OCH_2CH_3, $K_a = 1.24 \times 10^5$ M^{-1}) < **4** (4,4′-OC(=O)CH_3, $K_a = 1.26 \times 10^6$ M^{-1}). This selectivity arises from a combination of CH−π and CH···O=C interactions, which were found in the X-ray crystal structure of **4**@**3b** (Figure 2a and 2b). The electrostatic potential repulsion between the lone pair electron of the carbonyl oxygen atom of the ester group of **17**, which is inwardly directed toward the aromatic cavity of **3a**, and the electron-rich aromatic cavity of **3a** would be one of the reasons for the low encapsulation ability of **17** in **3a** compared with **4**−**6**.[19a]

Item 4. In a series of 4,4′-disubstituted-diphenylacetylene derivatives, the value of K_a of guest@**3a** in C_6D_6 increases in the order **16** (4,4′-Br, K_a = 245 M^{-1}) < **14** (4,4′-OCH_3, $K_a = 4.57 \times 10^3$ M^{-1}) < **15** (4,4′-I, $K_a = 8.71 \times 10^3$ M^{-1}). This result indicates that the CH···I interaction between the polarized inner proton of the methylene-bridge rim (O−C$H_{in}$$H_{out}$-O) of **3a** and the δ(−) equatorial region of the iodo atom in the C−I bond of **15** and the I···π interaction between the δ(+) polar region of the iodo group and the aromatic cavity of **3a** are effective for guest encapsulation.[18,19] The change in the ^{1}H NMR chemical shift ($\Delta\delta$) of the inner proton of the methylene-bridge rim of guest@**3a** relative to that of free **3a** in C_6D_6 ($CDCl_3$) was $\Delta\delta$ = 0.40 ppm (0.15 ppm) for **15** based on a CH···I interaction, $\Delta\delta$ = 0.26 (0.04) for **4** based on a CH···O=C interaction, and $\Delta\delta$ = 0.17 (−0.08) for **6**.

Item 5. Capsule **3a** strictly discriminates between a difference of one or two carbon atoms in guest size. In contrast to **5**, **6**, and **15** encapsulated in **3a**, guests **25**, **21**−**24**, and **26** were scarcely encapsulated, respectively. In a series of 4,4′-dialkynyl-biphenyl derivatives, the value of K_a of guest@**3a** in C_6D_6 increases in the order **20** < **18** < **19**. Thus, a fit between the guest and the cavity of **3a** in size is essential for encapsulation.[3g,18,19,26]

Thermodynamics of Guest@3a and the Solvent Effect. The thermodynamics of guest@**3a** in $CDCl_3$ and C_6D_6 were studied to elucidate the reasons for the difference in K_a of guest@**3a** in $CDCl_3$ and C_6D_6. Based on the value of K_a as a function of the temperature, the van't Hoff plots gave the thermodynamic parameters of the enthalpic ($\Delta H°$) and entropic ($\Delta S°$) contributions for guest encapsulation in **3a**.[17] The results are summarized in Table 2.[27] The following features (Items 1−4) are noteworthy regarding the thermodynamics of guest@**3a**.

(26) Mecozzi, S.; Rebek, J., Jr. *Chem.—Eur. J.* **1998**, *4*, 1016–1022.

Chart 1. Encapsulation and No Encapsulation Guests in **3a**

Encapsulation guests in **3a**

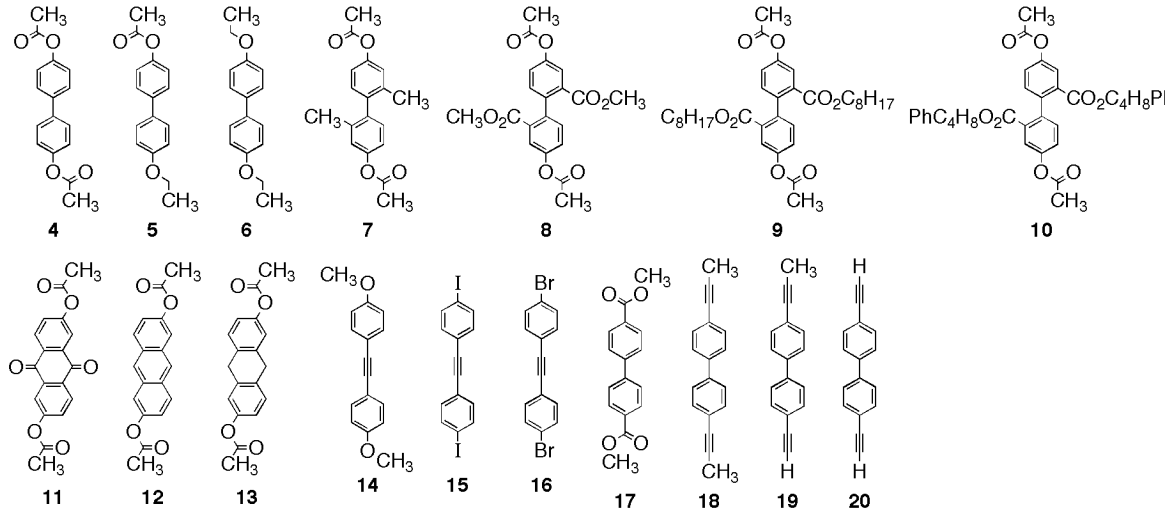

No encapsulation guests in **3a**

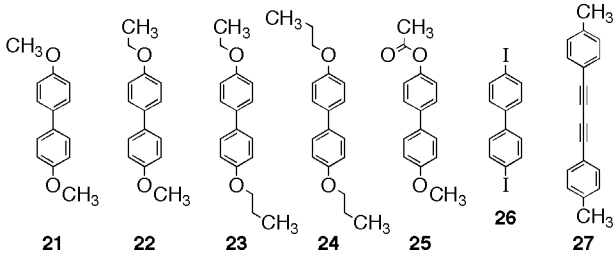

Table 1. Association Constants (K_a) of **3a** with Guests in $CDCl_3$ and C_6D_6,[a] and the ^1H NMR Chemical Shift Changes ($\Delta\delta_G$) of Guest@**3a** Relative to Free Guests at the Terminal Functional Groups[b]

guest	K_a (M^{-1}) in $CDCl_3$ at 298 K	$\Delta\delta_G$ (ppm)	K_a (M^{-1}) in C_6D_6 at 313 K	$\Delta\delta_G$ (ppm)	K_a(in C_6D_6)/K_a(in $CDCl_3$)
4[c,d]	81.7	−4.04	1.26×10^6	−2.85	1.54×10^4
5[c]	33.0	−4.08[e]	1.24×10^5	−2.86[e]	3.76×10^3
		−3.80[f]		−2.82[f]	
6[c]	8.1	−3.84	1.30×10^4	−2.87	1.61×10^3
7	53.1	−4.04	6.14×10^4	−2.99	1.16×10^3
8	44.2	−3.99	5.42×10^5	−2.81	1.23×10^4
9	22.2	−4.00	4.75×10^5	−2.79	2.14×10^4
10	13.4	−3.99	3.41×10^5	−2.80	2.54×10^4
11	224	−4.07	4.25×10^6	−2.73	1.90×10^4
12[c]	38.3	−4.11	1.83×10^6	−2.88	4.78×10^4
13	18.2	−4.05	2.12×10^5	−2.88	1.16×10^4
14	nd[g]		4.57×10^3	−2.20	
15	19.3	−0.33[h]	8.71×10^3	0.83[h]	450
16	nd[g]		245	1.14[h]	
17	nd[g]		567	−2.91	
18	nd[g]		507	−3.18	
19	nd[g]		2.71×10^3	−2.98[i]	
				−3.02[j]	
20	nd[g]		174[k]	−[k]	

[a] $K_a = [G@\mathbf{3a}]/\{[\mathbf{3a}]_f[G]_f\}$ or $K_a/K_{a\text{-Standard}} = \{[G@\mathbf{3a}][G_{Standard}]_f\}/\{[G_{Standard}@\mathbf{3a}][G]_f\}$. [b] $\Delta\delta_G = \delta_{encapsulated\text{-}guest} - \delta_{free\text{-}guest}$. [c] See ref 15. [d] The K_a of **3a** with **4** in CD_2Cl_2 at 298 K was 2.50×10^3 M^{-1} with $\Delta\delta_G = -4.00$ ppm. [e] Acetoxy group. [f] Ethoxy group. [g] Nd is not detected due to too small K_a. [h] Aromatic protons at 3(3′) and 5(5′) positions. [i] Propynyl group. [j] Ethynyl group. [k] See ref 25.

Item 1. The encapsulation of guests within **3a** in C_6D_6 are enthalpically driven with large values of K_a (entries 6−8), whereas the encapsulation of guests in $CDCl_3$ tended to be both enthalpically and entropically driven with small values of K_a (entries 1−5).

Table 2. Thermodynamic Parameters for the Encapsulation of Guests within **3a** in $CDCl_3$ and C_6D_6[a]

entry	guest	solvent	$\Delta H°$ (kcal mol^{-1})	$\Delta S°$ (cal mol^{-1} K^{-1})	$\Delta G°_{(298K)}$ (kcal mol^{-1})
1	**4**	$CDCl_3$	−1.87	2.25	−2.54
2	**8**	$CDCl_3$	1.31	11.92	−2.24
3	**11**	$CDCl_3$	−1.77	4.70	−3.17
4	**11**	sat. D_2O−$CDCl_3$	−0.97	7.36	−3.16
5	**7**	$CDCl_3$	−2.69	−0.93	−2.41
6	**7**	C_6D_6	−18.60	−38.97	−6.99
7	**6**	C_6D_6	−26.33	−65.18	−6.91
8	**14**	C_6D_6	−14.14	−28.47	−5.66

[a] $\Delta H°$ and $\Delta S°$ were obtained by van't Hoff plots: $\ln K_a = -(\Delta H°/R)(1/T) + (\Delta S°/R)$. $\Delta G°_{(298K)} = \Delta H° - T\Delta S°$, wherein $T = 298$ K.

Item 2. In a series of 4,4′-diacetoxybiphenyl derivatives with substituents at the 2,2′-positions in $CDCl_3$, the encapsulation of the relatively more polar guest **8** (2,2′-CO_2CH_3, entry 2) showed a major entropic contribution, whereas the encapsulation of the relatively less polar **7** (2,2′-CH_3, entry 5) indicated nearly an enthalpic contribution, and the encapsulation of the medium polarity **4** (2,2′-H, entry 1) exhibited both enthalpic and entropic contributions. Upon guest encapsulation, such as **8** in **3a**, a $CDCl_3$-solvated guest would release $CDCl_3$ molecules giving rise to an enhancement of the entropic contribution.[22a,28]

(27) To minimize experimental errors, in $CDCl_3$, guests **4**, **7**, **8**, and **11** were chosen, which showed large K_a values (44−224 M^{-1} at 298 K) among a series of guests@**3a** in $CDCl_3$. On the other hand, in C_6D_6, guests **6**, **7**, and **14** with moderate K_a values (4.6×10^3−6.1×10^4 M^{-1} at 313 K) were chosen among a series of guests@**3a** in C_6D_6. In C_6D_6, guests **4**, **8**, and **11** showed too large K_a values, and their K_a could not be determined directly but just by competitive encapsulation experiments.

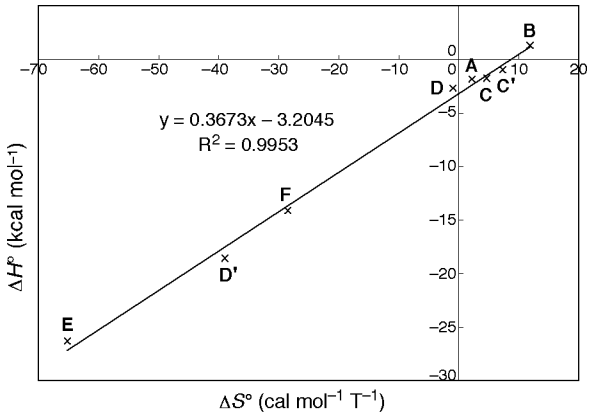

Figure 5. Plot of the enthalpy vs entropy values for the encapsulation of guests within **3a** in $CDCl_3$ and C_6D_6 based on the data of Table 2: (A) **4** in $CDCl_3$, (B) **8** in $CDCl_3$, (C) **11** in $CDCl_3$, (C′) **11** in sat. $D_2O-CDCl_3$, (D) **7** in $CDCl_3$, (D′) **7** in C_6D_6, (E) **6** in C_6D_6, and (F) **14** in C_6D_6.

However, the value of K_a of **8** with **3a** was not greater than that of **7** with **3a** in $CDCl_3$. This result suggests that $CDCl_3$ solvation of a guest would not contribute strongly to an increase of K_a.

Item 3. Guest encapsulation in D_2O-saturated $CDCl_3$ enhances the trend toward entropic contribution compared with that in $CDCl_3$ (entry 4 vs entry 3). However, under both conditions, the value of K_a was almost the same.

Item 4. Based on the thermodynamic parameters for the encapsulation of guests within **3a** in $CDCl_3$ and C_6D_6 shown in Table 2, the encapsulation process shows an enthalpy−entropy compensation effect (Figure 5).[28]

The small value of K_a and considerable entropic contribution for guest@**3a** in $CDCl_3$ suggest that $CDCl_3$ acts as a guest competitor for **3a**. Several molecules of $CDCl_3$ may be encapsulated in **3a** or may interact with the inner aromatic cavity of **3a**,[29] and upon encapsulation of guest into **3a**, the encapsulated $CDCl_3$ molecules would be released from the cavity of **3a** to give a positive $\Delta S°$.[30] When pure **4**@**3a**, prepared in benzene and dried in vacuo, was dissolved in $CDCl_3$, the release of **4** from **4**@**3a** into the bulk phase of $CDCl_3$ occurred immediately at 296 K. The ratio of **4**@**3a**:free-**3a** was 60:40 after 3 min and 48:52 after 24 h, reaching an equilibrium.[15] In C_6D_6, which is less polar than $CDCl_3$, noncovalent interactions between the guests and the inner cavity of capsule **3a**, such as CH−π and CH···O═C interactions, would work more effectively, leading to a significant enthalpic contribution and a large value of K_a in C_6D_6. The value of K_a of as-prepared **3a** with **4** in CD_2Cl_2 was compared with the value of K_a in $CDCl_3$ and C_6D_6.[17] The value of K_a of **3a** with **4** in solvents increased in the order $CDCl_3$ (82 M^{-1} at 298 K) < CD_2Cl_2 (2.50×10^3 M^{-1} at 298 K) < C_6D_6 (1.26×10^6 M^{-1} at 313 K), whereas the dielectric constant increases in the order C_6H_6 (2.28) < $CHCl_3$ (4.81) < CH_2Cl_2 (8.93). This result also indirectly supports the assertion that $CDCl_3$ acts as a guest competitor for **3a**. $CDCl_3$ is larger than CD_2Cl_2 in size, and the CD···π and Cl···π interactions[18,19] between the solvent and the aromatic cavity of **3a** would be more favorable for $CDCl_3$ than for CD_2Cl_2 based on the difference in the number of electronegative Cl atoms.

Table 3. Molar Ratio of **28** and **30** at 298 K in the Reaction Mixture after Heating a 1:1 Mixture of **28** and **29** To Form **30** in $CDCl_3$ and C_6D_6 at 323 K for 12 h[a]

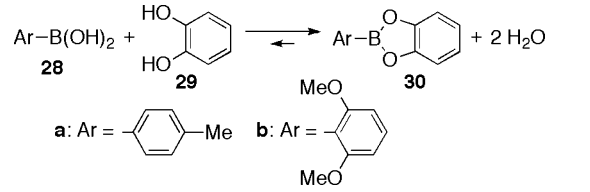

entry	Ar	solvent	**28**:**30**
1	**a**	$CDCl_3$	2.0:98.0
2	**a**	C_6D_6	5.9:94.1
3	**a**	$CDCl_3-D_2O$[b]	9.5:90.5
4	**a**	$C_6D_6-D_2O$[b]	15.1:84.9
5	**b**	$CDCl_3$	72.7:27.3
6	**b**	C_6D_6	83.9:16.1
7	**b**	$CDCl_3-D_2O$[b]	98.9:1.1
8	**b**	$C_6D_6-D_2O$[b]	97.3:2.7

[a] $[\mathbf{28}]_i = [\mathbf{29}]_i = 17$ mM in solvent (600 μL).[31] [b] To a solution of the resulting reaction mixture (entries 1, 2, 5, and 6) were added 5 μL of D_2O (27 equiv), and the mixture was heated again at 323 K for 12 h.

Solvent Effect on the Thermodynamic Stability of Arylboronic Acid Catechol Esters. As a model for studying the thermodynamic stability of the boronic ester bond of **3a**, the reaction of arylboronic acids **28** with catechol **29** to produce the arylboronic acid catechol esters **30** was investigated in $CDCl_3$ and C_6D_6. The results are summarized in Table 3.

The ^1H NMR spectra of the reaction mixture of 4-methylphenylboronic acid **28a** with **29** (17 mM each) in $CDCl_3$ and C_6D_6 at 298 K after heating at 323 K for 12 h showed a mixture of **28a** and its catechol ester **30a** in ratios of 2.0:98.0 and 5.9:94.1, respectively.[17,31] Upon addition of 5 μL (27 equiv) of D_2O to these mixtures and then reheating at 323 K for 12 h, the equilibrium ratio of **28a** and **30a** shifted to 9.5:90.5 in $CDCl_3$ and 15.1:84.9 in C_6D_6 at 298 K. On the other hand, the reaction of 2,6-dimethoxyphenylboronic acid **28b** with **29** under the same conditions gave a mixture of **28b** and **30b** in a ratio of 72.7:27.3 in $CDCl_3$ and 83.9:16.1 in C_6D_6.[17,31] On addition of D_2O and reheating under the same conditions, **30b** was almost hydrolyzed back into **28b** in both $CDCl_3$ and C_6D_6. These results clearly indicate that (1) the arylboronic acid catechol esters **30a** and **30b** are thermodynamically more stable in $CDCl_3$ than in C_6D_6 and (2) **30b** is less stable than **30a** is, which is probably the result of the near orthogonal conformation between the aryl group and the catecholatoboryl plane of **30b** with respect to the coplanar conformation of **30a**.

Thus, the fact that arylboronic acid catechol esters **30** are thermodynamically more stable in $CDCl_3$ than in C_6D_6 also

(28) Leung, D. H.; Bergman, R. G.; Raymond, K. N. *J. Am. Chem. Soc.* **2008**, *130*, 2798–2805.

(29) In the ^1H NMR spectra of **3a** in $CHCl_3$ even at 218 K with $CDCl_3$ sealed in a capillary for NMR deuterium-locking or a mixture of **3a** and 100 equiv of $CHCl_3$ in C_6D_6, no signal of $CHCl_3$ encapsulated in **3a** was observed. These results suggest a small K_a and very fast exchange of $CHCl_3$ in and out of **3a** on the NMR time scale.

(30) (a) Kang, J.; Rebek, J., Jr. *Nature* **1996**, *382*, 239–241. (b) Yamanaka, M.; Shivanyuk, A.; Rebek, J., Jr. *J. Am. Chem. Soc.* **2004**, *126*, 2939–2943.

(31) The ^1H NMR spectra of **28a** (17 mM) in $CDCl_3$ and C_6D_6 at 298 K showed a mixture of **28a** and its boroxine (trimeric anhydride of **28a**) in ratios of 36.8:63.2 and 61.1:38.9, respectively, after 30 min of dissolution.[17] After reaching an equilibrium in 36 h at 298 K, the ratio of **28a** and its boroxine was 43.5:56.5 in $CDCl_3$ and 60.0:40.0 in C_6D_6. This result indicates that the boroxine is thermodynamically more stable in $CDCl_3$ than in C_6D_6. Upon addition of **29** to this mixture, the boroxine almost disappeared to produce **30a** concomitantly with **28a**. In contrast, **28b** (17 mM) remained intact in both $CDCl_3$ and C_6D_6 and its boroxine was not detected even after heating at 323 K for 12 h.[17]

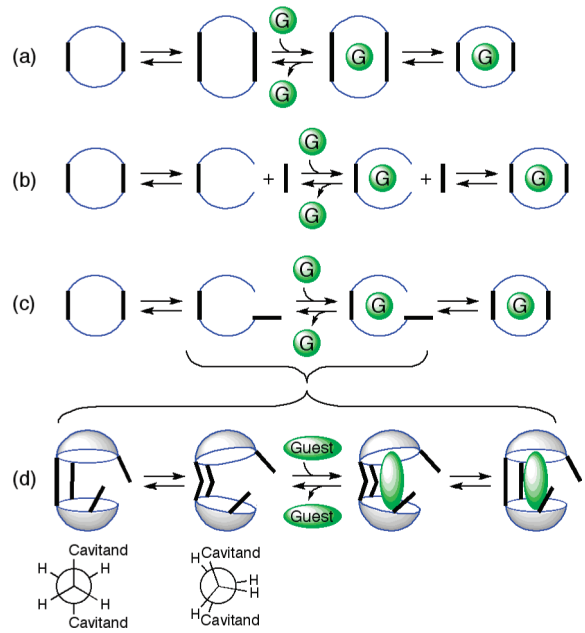

Figure 6. Schematic representations of possible mechanisms for the guest encapsulation and release into and out of **3a**: (a) an extended portal mechanism, (b) a linker dissociation mechanism, and (c) a linker partial dissociation mechanism. (d) Conformational change of the two linkers connected with the two cavitands from anti to eclipsed-like conformation.

indirectly supports that the small K_a value for guest@**3a** in $CDCl_3$ compared with that in C_6D_6 does not arise from the difference in stability of the boronic ester bonds of **3a** in $CDCl_3$ and C_6D_6, but probably from the character of $CDCl_3$ as a guest competitor for **3a**.

Mechanism of Guest Encapsulation in 3a: A Kinetic Study. Capsule **3a** is composed of two molecules of tetrakis(dihydroxyboryl)-cavitand **1a** as a polar aromatic cavity and four molecules of 1,2-bis(3,4-dihydroxyphenyl)ethane **2** as an equatorial bis(catechol)-linker connected by eight dynamic boronic ester bonds. Three mechanisms are possible for guest encapsulation in capsule **3a** (Figure 6).

The first mechanism is an extended portal mechanism based on a conformational change of the linker **2** unit (Figure 6a).[22a] However, the following facts rule out this mechanism. In the crystal structure of **4@3b**, all linkers adopt an approximate *anti*-conformation, although they are highly disordered, even at 100 K, and are not necessarily arranged in the same direction (Figure 2). The *anti*-conformation of the linker is the most extended form between two catechol moieties among all the possible conformations. Therefore, it is no longer possible for **3a** to extend the equatorial portal. In fact, the dimension of the equatorial portal of **3b** in the crystal structure, in which **3b** was observed as an average form between the twistomers and slipped forms, was almost the same as that in the calculated twisted form of **3** (vide supra). The intact portal at the equatorial position of **3a** is not large enough to allow guest molecules as large as **4** and **8** to enter and egress the inner phase of capsule **3a**, as shown in Figures 2a, 2b, and 4d.

Consideration of a CPK model suggests that a *complete or partial dissociation of the two linkers from* **3a** (Figure 6b or 6c), *followed by the conformational change of the remaining two linkers connected with the two cavitands from the anti to eclipsed-like conformation* (Figure 6d) is required for the opening of the equatorial portal of **3a**, followed by the ingression

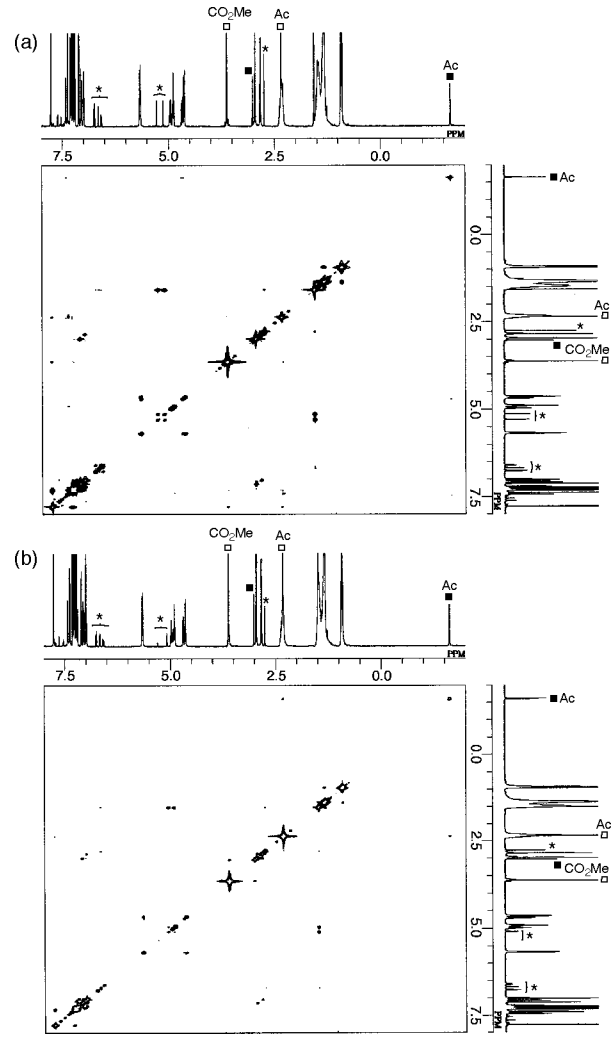

Figure 7. Variable temperature 2D NOESY spectra of a mixture of as-prepared **3a**, **8**, and free **2** in $CDCl_3$ under the conditions of [**3a**] = 2.5 mM, [**8**] = 12.5 mM, and [**2** (saturated)] = 0.94 mM, pulse delay = 3.0 s, and mixing time = 1.0 s: (a) at 298 K and (b) at 323 K. The representative signals of **8** of **8@3a** and free **8** are marked with solid and open squares, respectively. The signals of free **2** are marked with asterisks.

of a guest into **3a** and its egression out of **3a**. A catalytic amount of adventitious water leading to the reversibility of boronic ester bond is inevitably present in $CDCl_3$ and C_6D_6.

However, a linker dissociation mechanism, wherein two of the four linkers completely dissociate from **3a** (Figure 6b) would not be also plausible based on the following results. In the 2D NOESY spectra of a mixture of as-prepared **3a** (2.5 mM), 5 equiv of **8**, and 0.38 equiv of free **2** in $CDCl_3$,[32] exchange cross-peaks between **8@3a** and free **2**, between guest-free **3a** and free **2**, and between **8@3a** and free **8** were not observed below 308 K, even for a mixing time of 1.0 s (Figure 7a). At 323 K, exchange cross-peaks between **8@3a** and free **2** and between guest-free **3a** and free **2** were also not observed, whereas exchange cross-peaks between **8@3a** and free **8** were observed in $CDCl_3$ (Figure 7b). These results indicate that (1) the linker exchange of **3a** is much slower than the guest-exchange rate or (2) the complete dissociation of the two linkers from **3a** does not occur on an NMR time scale.

(32) The saturated concentration of free **2** was 0.28 and 0.94 mM in $CDCl_3$ at 298 and 323 K, respectively, and 0.19 and 0.90 mM in C_6D_6 at 298 and 323 K, respectively, based on the ^{1}H NMR integration ratio with *p*-dimethoxybenzene as an internal standard.

The most plausible mechanism for guest encapsulation and release into and out of **3a** is a linker partial dissociation mechanism (Figure 6c),[7a] wherein dissociation of each one of the respective two boronic ester bonds of the two linkers among the four linkers of **3a** occurs. Two opposite or adjacent linkers among the four linkers would open up the capsule (the partial dissociation of two adjacent linkers is depicted in Figure 6c and 6d).[33] If this linker partial dissociation mechanism is correct, then the linker exchange of **3a** would not be observed in its 2D NOESY spectrum. The reversible mechanism shown in Figure 6c and 6d is composed of three steps. The first step is a linker partial dissociation to give a gate-opening guest-free **3a** (the following parentheses denote the gate-opening guest@**3a** step as the reverse reaction). The second step is the guest uptake into the gate-opening **3a** (or guest release out of the gate-opening guest@**3a**) that occurs simultaneously with the conformational change of the two linkers connected with the two cavitands from the anti to the eclipsed-like conformation. The final step is a linker reassociation and gate-closing process to form guest@**3a** (or guest-free **3a**). To elucidate this mechanism, the pseudo-first-order exchange rate constants for release (k_{-1}) and encapsulation (k_1) of the guest from and into **3a**, respectively, and second-order rate constant of guest encapsulation ($k_1^* = k_1$/[guest]) in $CDCl_3$ and in C_6D_6 were determined from a 2D EXSY analysis based on the integration values of the exchange cross-peaks and diagonal peaks of the encapsulated and free guests in the 2D NOESY spectra (Figures 7 and 8).[17,30b,34] The results, together with the calculated free energy of activation ($\Delta G_{-1}^{\ddagger}$, $\Delta G_1^{\ddagger}$, and $\Delta G_1^{*\ddagger}$), are summarized in Table 4.[35] There are several features in the kinetic study shown in Table 4.

Item 1. For **8**, the value of k_1 increases with guest concentration, and the values of k_1^* and k_{-1} are roughly independent of guest concentration for both $CDCl_3$ and C_6D_6 (entries 1, 2, and 4, and 5, 7, and 8, respectively).

Item 2. The external addition of linker **2** to a solution of **3a** and **8** barely increases the value of k_1 (k_1^*) and k_{-1} for both $CDCl_3$ and C_6D_6 (entries 2 vs 3, and 5 vs 6, respectively).

Item 3. For **8**, **5**, and **6** in C_6D_6, both the values of k_1 (k_1^*) and k_{-1} increase in the order **8** < **5** < **6**, indicating a significant dependency on the characteristics of the guest molecule (entries 5 vs 10, and 9 vs 11, respectively). This order could be related to the difference in size of the guest functional groups or the interaction ability of them with **3a** (or partially dissociated **3a**), such as hydrogen bonding and CH$-\pi$ interactions.

Item 4. For **8**, the value of k_1 (k_1^*) and k_{-1} in C_6D_6 is apparently greater than the value of k_1 (k_1^*) and k_{-1} in $CDCl_3$ (entries 1 vs 5, 2 vs 7, and 4 vs 8, respectively). Namely, $\Delta G_1^{\ddagger}$ ($\Delta G_1^{*\ddagger}$) and $\Delta G_{-1}^{\ddagger}$ in $CDCl_3$ are higher than those in C_6D_6.

The results in Items 1−3 indicate that the guest uptake in **3a** follows second-order kinetics and the guest release out of **3a** follows first-order kinetics,[30b] and suggest the linker partial dissociation mechanism. Item 4 may reflect the solvation effect

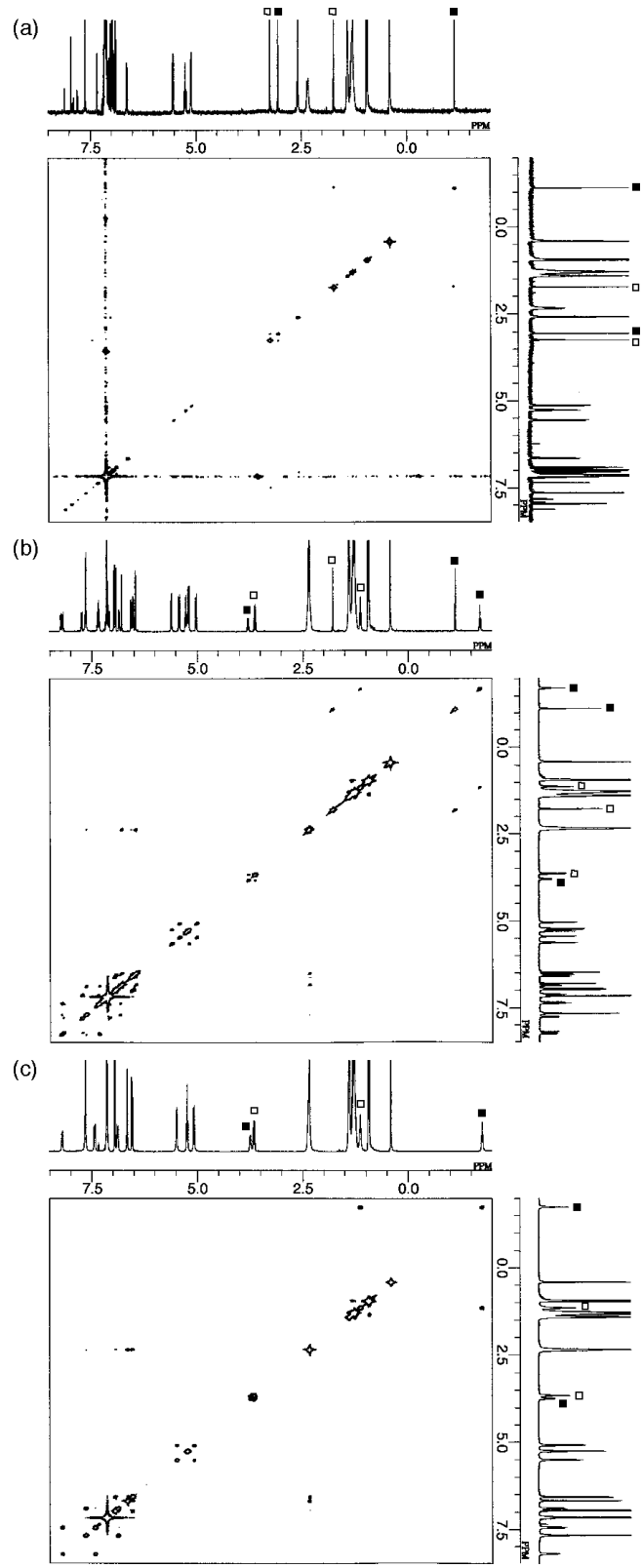

Figure 8. 2D NOESY spectra of a mixture of **3a** and guests in C_6D_6 for 2D EXSY analysis under the conditions of pulse delay = 3.0 s, and mixing time = 1.0 s: (a) [**3a**] = 0.5 mM, [**8**] = 1.0 mM at 323 K, (b) [**3a**] = 2.5 mM, [**5**] = 5.0 mM at 313 K, and (c) [**3a**] = 2.5 mM, [**6**] = 5.0 mM at 313 K. The representative signals of guest of guest@**3a** and free guest are marked with solid and open squares, respectively.

(33) Craig, S. L.; Lin, S.; Chen, J.; Rebek, J., Jr. *J. Am. Chem. Soc.* **2002**, *124*, 8780–8781.

(34) (a) Abel, E. W.; Coston, T. P. J.; Orrell, K. G.; Sik, V.; Stephenson, D. *J. Magn. Reson.* **1986**, *70*, 34–53. (b) Pons, M.; Millet, O. *Prog. Nucl. Magn. Reson. Spectrosc.* **2001**, *38*, 267–324.

(35) Guests **5**, **6**, and **8** were chosen for the 2D EXSY analysis because the diagonal peaks of encapsulated and free guests in the 2D NOESY spectra did not overlap with each other or those of the capsule **3a**. However, when excess amounts of guests were used, those faintly overlapped with each other in some cases, increasing experimental errors for k_1 and k_{-1}. The use of excess amounts of guests or low **8**@**3a**/free-**8** would produce a large difference in integration values between the diagonal peak of the free guest and the exchange cross-peak, also increasing experimental errors for k_1 and k_{-1}. Note that the values of k_1 and k_{-1} contain an experimental error of 10%−15%.

Table 4. Pseudo-First-Order Exchange Rate Constants for Release (k_{-1}) and Encapsulation (k_1) of Guests from and into Capsule **3a**, Respectively, and Second-Order Rate Constant of Guest Encapsulation ($k_1^* = k_1$/[guest]) in $CDCl_3$ and in C_6D_6,[a] and Free Energy of Activation of Release ($\Delta G_{-1}^{\ddagger}$) and Encapsulation ($\Delta G_1^{\ddagger}$, $\Delta G_1^{*\ddagger}$) of Guest@**3a**[b]

entry	guest	solvent	[G]/[**3a**][c]	T (K)	k_{-1} (s^{-1})	k_1 (s^{-1})	k_1^* (s^{-1} M^{-1})	$\Delta G_{-1}^{\ddagger}$ (kcal mol^{-1})	$\Delta G_1^{\ddagger}$ (kcal mol^{-1})	$\Delta G_1^{*\ddagger}$ (kcal mol^{-1})
1	**8**	$CDCl_3$	2	323	0.002	0.034	6.80	22.9	21.1	17.7
2	**8**	$CDCl_3$	5	323	0.002	0.076	6.08	22.9	20.6	17.8
3	**8**	$CDCl_3$	5[d]	323	0.005	0.099	7.92	22.3	20.4	17.6
4	**8**	$CDCl_3$	10	323	0.007	0.157	6.28	22.1	20.1	17.8
5	**8**	C_6D_6	2	323	0.013	0.044	44.0	21.7	20.9	16.5
6	**8**	C_6D_6	2[d]	323	0.016	0.035	35.0	21.6	21.1	16.7
7	**8**	C_6D_6	5	323	0.017	0.097	38.8	21.6	20.4	16.6
8	**8**	C_6D_6	10	323	0.018	0.238	47.6	21.5	19.9	16.5
9	**5**	C_6D_6	2	313	0.120	0.207	41.4	19.7	19.3	16.0
10	**5**	C_6D_6	2	323	0.342	0.537	107	19.6	19.3	15.9
11	**6**	C_6D_6	2	313	0.836	2.46	493	18.5	17.8	14.5

[a] Pseudo-first-order exchange rate constants (k_{-1}, k_1) were estimated by 2D EXSY experiments. [b] $\Delta G_{-1}^{\ddagger} = -RT \ln(hk_{-1}/k_BT)$, $\Delta G_1^{\ddagger} = -RT \ln(hk_1/k_BT)$, and $\Delta G_1^{*\ddagger} = -RT \ln(hk_1^*/k_BT)$. [c] [G]/[**3a**] = [guest]/[**3a**]; [**3a**] = 2.5 mM for **8**@**3a** in $CDCl_3$, **5**@**3a** in C_6D_6, and **6**@**3a** in C_6D_6; and [**3a**] = 0.5 mM for **8**@**3a** in C_6D_6. [d] Linker **2** was added (saturated concentration of **2** at 323 K: 0.94 mM in $CDCl_3$ and 0.90 mM in C_6D_6).

of the guest, **3a** (guest@**3a**), or the partially linker-dissociated **3a** (guest@**3a**).

It is known that the stability of hemicarceplexes formed between covalently bonded hemicarcerands and their guests is governed by two free energy terms: the intrinsic binding (free energy of complexation, thermodynamic $\Delta G°$) and the constrictive binding (free energy of activation for complex formation, kinetic $\Delta G^{\ddagger}_{association} - \Delta G^{\ddagger}_{dissociation}$),[1c,22,36] wherein the balance of the free energy is $(\Delta G^{\ddagger}_{association} - \Delta G^{\ddagger}_{dissociation}) \approx \Delta G°$. However, this is not true in the case of guest@**3a**, wherein the balance of the free energy for **8**@**3a** in $CDCl_3$ at 323 K (entry 2) was $(\Delta G_1^{*\ddagger} - \Delta G_{-1}^{\ddagger}) = -5.1$ kcal/mol $< \Delta G° = -2.5$ kcal/mol, and the balance of the free energy for **8**@**3a** in C_6D_6 (entry 7) was $(\Delta G_1^{*\ddagger} - \Delta G_{-1}^{\ddagger}) = -5.0$ kcal/mol at 323 K $> \Delta G° = -8.2$ kcal/mol at 313 K. The difference between $(\Delta G_1^{*\ddagger} - \Delta G_{-1}^{\ddagger})$ and $\Delta G°$ in guest@**3a** may reflect the linker partial dissociation, as well as the solvation effect.

The linker partial dissociation mechanism shown in Figure 6c also facilitates the understanding of the mechanism of the interconversion between the (*M*)- and (*P*)-twisted forms (racemic twistomers) through the slipped forms in **3a** (Figures 9 and 2f). In one linker **2** unit in **3a**, one boronic ester bond dissociation and a subsequent rotation of the CH_2-Ar bond and the reformation of the boronic ester, followed by a progression of the same process for the other boronic ester moiety, would complete the interconversion of the (*M*)- to the (*P*)-form for one linker (Figure 9). Application of the same process to the other three linkers would complete the interconversion of the (*M*)- to the (*P*)-form of **3a** through an intramolecular mixture of (*M*)- and (*P*)-forms of the four linkers in **3a** (Figure 2f).

Guest Rotation within 3a. Molecular gyroscopes have attracted considerable attention in the field of mechanical molecular devices.[37,38] They consist of a rotator with a spinning axis and a stator framework, wherein the rotator is encased and protected by a stator. So far, molecular gyroscopes have been synthesized using several types of covalent-bond strategies[38,39] or by a metal-coordination strategy, such as a metal-centered

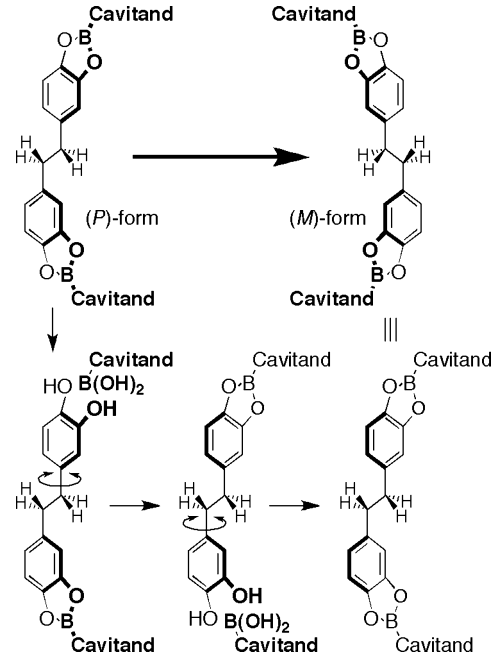

Figure 9. Schematic representation for the interconversion of one linker **2** unit in **3a**.

gyroscope.[40] Recently, it has been reported that a self-assembled molecular capsule with an encapsulated guest behaves as a supramolecular gyroscope, in which an encapsulated guest is the rotator and a self-assembled capsule is the stator.[2k,41]

To explore the capability of guest@**3a** as a supramolecular gyroscope, the rotation behavior of 4,4′-diacetoxy-2,2′-disubstituted-biphenyls **8**−**10** within **3a** was investigated. Guests **8**−**10** were oriented with their long axis aligned along the long axis of **3a**, as mentioned above, and can rotate along this axis within **3a**. The inner and outer protons of the methylene-bridge

(36) (a) Houk, K. N.; Nakamura, K.; Sheu, C.; Keating, A. E. *Science* **1996**, *273*, 627–629. (b) Yoon, J.; Cram, D. J. *Chem. Commun.* **1997**, 1505–1506.
(37) (a) Kottas, G. S.; Clarke, L. I.; Horinek, D.; Michl, J. *Chem. Rev.* **2005**, *105*, 1281–1376. (b) Kay, E. R.; Leigh, D. A.; Zerbetto, F. *Angew. Chem., Int. Ed.* **2007**, *46*, 72–191.
(38) Khuong, T.-A. V.; Nunez, J. E.; Godinez, C. E.; Garcia-Garibay, M. A. *Acc. Chem. Res.* **2006**, *39*, 413–422.
(39) (a) Bedard, T. C.; Moore, J. S. *J. Am. Chem. Soc.* **1995**, *117*, 10662–10671. (b) Dominguez, Z.; Dang, H.; Strouse, M. J.; Garcia-Garibay, M. A. *J. Am. Chem. Soc.* **2002**, *124*, 2398–2399. (c) Setaka, W.; Ohmizu, S.; Kabuto, C.; Kira, M. *Chem. Lett.* **2007**, *36*, 1076–1077. (d) Nuñez, J. E.; Natarajan, A.; Khan, S. I.; Garcia-Garibay, M. A. *Org. Lett.* **2007**, *9*, 3559–3561.
(40) (a) Shima, T.; Hampel, F.; Gladysz, J. A. *Angew. Chem., Int. Ed.* **2004**, *43*, 5537–5540. (b) Narwara, A. J.; Shima, T.; Hampel, F.; Gladysz, J. A. *J. Am. Chem. Soc.* **2006**, *128*, 4962–4963.
(41) Scarso, A.; Onagi, H.; Rebek, J., Jr. *J. Am. Chem. Soc.* **2004**, *126*, 12728–12729.

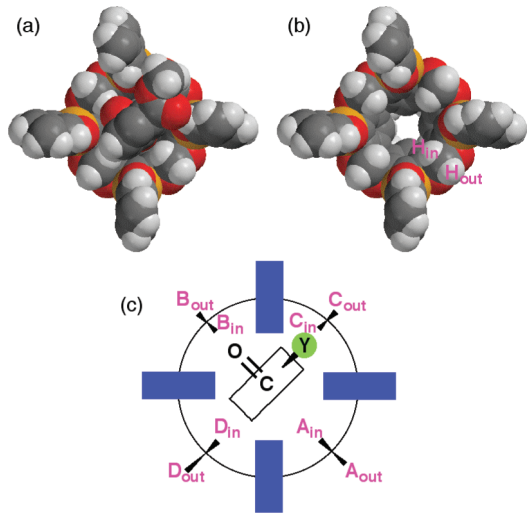

Figure 10. Top views of half-structure model of **3** (a) with and (b) without guest **8**. (c) Four-site model for the encapsulated-guest rotation along the long axis of **3a**, wherein schematic representation of the cross section of guest@**3a** is shown. The centered rectangle and the Y represent the half-biphenyl ring and the ester group of guests **8**−**10**, respectively. The C═O means the carbonyl moiety of the guest acetoxy group. The peripheral circle and rectangles represent the aromatic cavity of the **1a** unit and the catechol rings of the **2** unit in capsule **3a**, respectively. The A_{in}, B_{in}, C_{in}, and D_{in} (A_{out}, B_{out}, C_{out}, and D_{out}) represent the relative positions of the inner protons H_{in} (outer protons H_{out}) of the methylene-bridge rim of the **1a** unit of **3a** with respect to the positions of the carbonyl moiety and the substituent-Y of the encapsulated-guest rotating in **3a**.

rims (O−$CH_{in}H_{out}$−O) of **3a** act as molecular probes for the encapsulated-guest rotation within **3a**.[2k] Figure 10 depicts a four-site model for the encapsulated-guest rotation along the long axis of **3a**. In this model, if the encapsulated-guest rotation along the long axis of **3a** is too fast on the NMR time scale, then the ^{1}H NMR signals of the inner and outer protons (H_{in} and H_{out}) would appear as a respective one doublet signal, i.e., as the averaged form. In contrast, if the encapsulated-guest rotation is slow on the NMR time scale or comes to a stop, then the doublet signals of H_{in} and H_{out} would split into four sets of doublet signals with an integration ratio of A_{in}:B_{in}:C_{in}:D_{in} (A_{out}:B_{out}:C_{out}:D_{out}) = 1:1:1:1.

Figure 11 shows the ^{1}H NMR spectra of guest@**3a** (Y = CO_2CH_3 in **8**, Y = $CO_2(CH_2)_7CH_3$ in **9**, and Y = $CO_2(CH_2)_4Ph$ in **10**) in C_6D_6 at various temperatures.[17] This gave significant information on the encapsulated-guest rotation along the long axis of capsule **3a**, namely, of the rotational steric barrier effect for guests within **3a**. In the ^{1}H NMR spectrum of **8**@**3a** at 298 K (Figure 11a), the inner (H_{in}) and outer (H_{out}) protons of the methylene-bridge rims of **3a** appear as respective one sharp doublet signal. This spectrum remained unchanged, even at 213 K in $C_6D_5CD_3$.[17] This result undoubtedly indicates that the rotation of **8** within **3a** is too fast on the NMR time scale, even at 213 K. On the other hand, the ^{1}H NMR signals of H_{in} and H_{out} of **10**@**3a** were extremely broad and nearly coalesced at 298 K (Figure 11b) and were still broadened, even at 343 K (Figure 11c). In marked contrast, the ^{1}H NMR signals of H_{in} and H_{out} of **9**@**3a** at 298 K were split into four sets of doublet signals of A_{in}, B_{in}, C_{in}, and D_{in}, and A_{out}, B_{out}, C_{out}, and D_{out} in an integration ratio of 1:1:1:1, respectively (Figures 11d and 10c). These signals were nearly coalesced at 343 K (Figure 11f). This result clearly indicates that the rotation of **9** within **3a** is very slow on the NMR time scale at 298 K. Thus, the guest rotation within **3a** increases in the order **9** < **10** ≪ **8**. Namely,

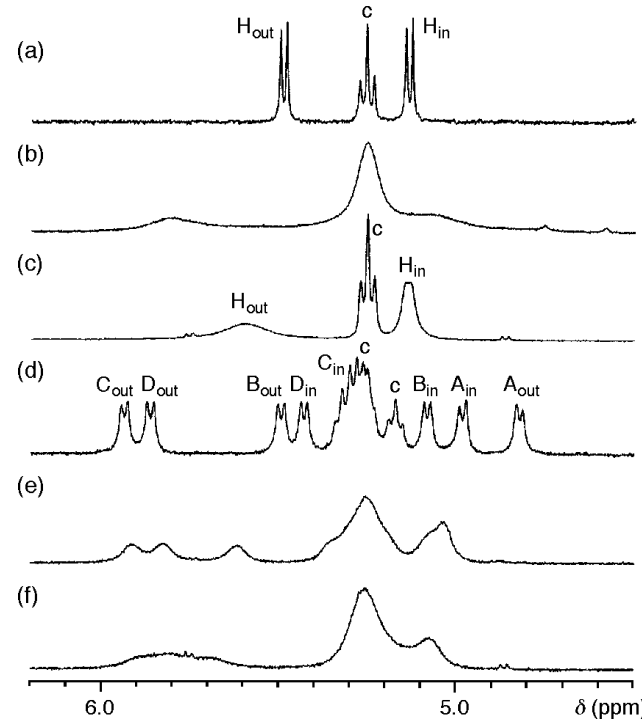

Figure 11. Guest-rotation behavior within **3a**, monitored by ^{1}H NMR (400 MHz, C_6D_6, [**3a**] = 2.5 mM and [guest] = 5 mM) in the region of the inner (H_{in}) and outer (H_{out}) protons of the methylene-bridge rims (O−$CH_{in}H_{out}$−O) of **3a**: (a) **8**@**3a** at 298 K, (b) **10**@**3a** at 298 K, (c) **10**@**3a** at 343 K, (d) **9**@**3a** at 298 K, (e) **9**@**3a** at 323 K, and (f) **9**@**3a** at 343 K. The signals marked 'A_{in}−D_{in}' and 'A_{out}−D_{out}' are assigned in Figure 10. The signal marked 'c' is assigned in Scheme 1.

the elongation of the ester group at the 2,2′-positions of 4,4′-diacetoxybiphenyl guests puts the brakes on guest rotation within **3a**.

Figure 12 shows the 2D NOESY spectrum of a 1:1 mixture of **9**@**3a** and free **9** in C_6D_6 at 298 K (mixing time = 0.5 s), wherein the guest exchange into and out of **3a** was not observed, and the acetoxy signal of the encapsulated **9** showed NOE correlations with four split inner protons (A_{in}−D_{in}) of the methylene-bridge rim of **3a** (Figure 12a). Furthermore, it should be noted that all the inner protons (A_{in}−D_{in}) and all the outer protons (A_{out}−D_{out}) of **3a** showed exchange cross-peaks with one another in addition to the NOE correlations (Figure 12b). For example, signal A_{in} showed an NOE correlation with A_{out} and exhibited exchange cross-peaks with B_{in}, B_{out}, C_{in}, C_{out}, D_{in}, and D_{out}. Similar correlations were also observed in $C_6D_5CD_3$ at 298 K (Figure 13a). This result shows that **9** within **3a** rotates at 298 K, although the rotation is slower than the NMR time scale. In marked contrast, at 243 K, only NOE correlations between the inner and outer protons were observed, and exchange cross-peaks were no longer observed (Figure 13c vs 13a), although the chemical shift of the inner and outer protons of **9**@**3a** changed depending on the solvent used and the temperature (Figures 12 and 13). This result clearly indicates that the rotation of **9** within **3a** ceases at 243 K.

Variable low temperature ^{1}H NMR spectra of **9**@**3a** and **10**@**3a** showed that four sets of doublet signals of the inner (A_{in}−D_{in}) and outer (A_{out}−D_{out}) protons of the methylene-bridge rims of **3a** were shifted, coalesced, and split at several points, depending on the temperature.[17] This result suggests that the guest rotation within **3a**, the interconversion of the twistomers of **3a**, and the internal rotation of the biphenyl moiety of the

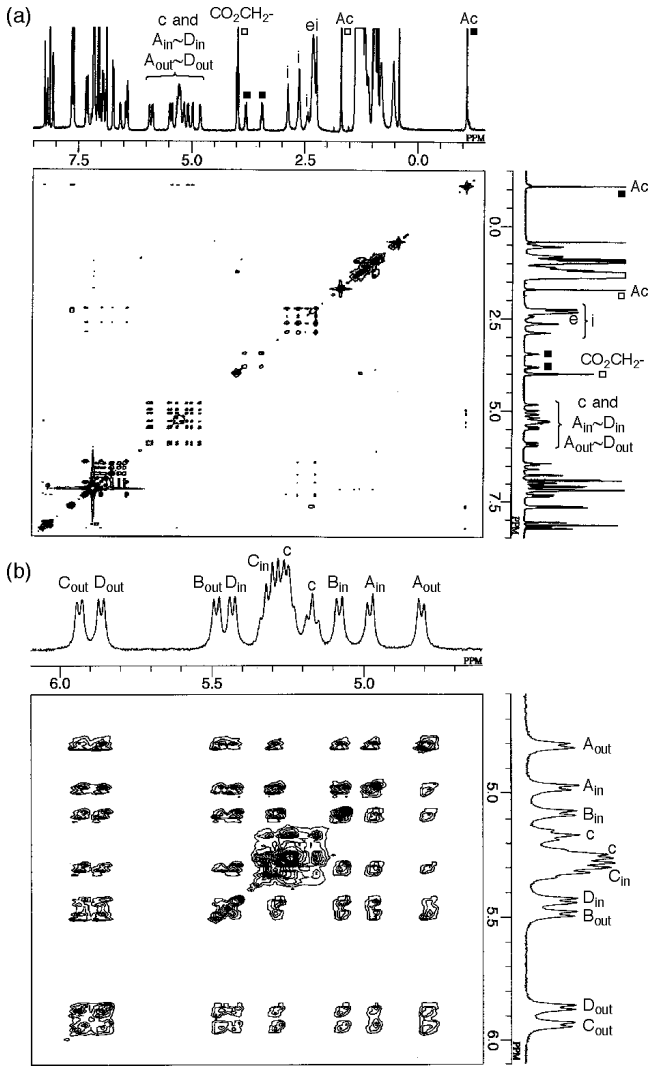

Figure 12. 2D NOESY spectrum of **9@3a** in C_6D_6 at 298 K (400 MHz, [**3a**] = 2.5 mM and [**9**] = 5 mM, pulse delay = 1.5 s, and mixing time = 0.5 s) in the regions (a) between −1.5 and 8.5 ppm and (b) between 4.6 and 6.2 ppm. The signals marked 'A_{in}−D_{in}' and 'A_{out}−D_{out}' are assigned in Figure 10. The signals marked 'c', 'e', and 'i' are assigned in Scheme 1. The solid and open squares indicate the representative signals of **9** of **9@3a** and free **9**, respectively.

guest coexist in cooperation with each other. Given this complexity, we could not determine the exchange rate constant for guest rotation within **3a** at this stage.

In **4@3a** in C_6D_6 or $C_6D_5CD_3$, the ^{1}H NMR signal of the ethylene moiety of the linker **2** unit of **3a** appeared as a single sharp singlet at 298 K, and this broadened without splitting, even at 213 K.[17] On the other hand, the linker signal of **8@3a** in $C_6D_5CD_3$ appeared as a multiplet at 298 K and split into two multiplets at 263 K.[17] In marked contrast, the linker signal of **9@3a** in C_6D_6 or $C_6D_5CD_3$ split into five signals at 298 K (three major broad signals and two minor broad signals, with one of the minor signals overlapping one of the major signals, Figures 12a and 14c). Furthermore, at least one of the three major signals split into two signals at 233 K.[17] In **9@3a**, the ^{1}H NMR signal of the α-protons of the octyl ester group ($CO_2-CH_2(CH_2)_6CH_3$) of the encapsulated **9** split into two sets of double triplet signals with an upfield shift relative to the triplet signal of the α-protons of free **9** (Figure 14c vs 14b).[42] This arises from the desymmetrization of the two geminal α-protons given the emergence of a chiral axis (racemization) in the encapsulated **9**, because the internal rotation of the biphenyl moiety of **9** is slow on the NMR time scale on encapsulation in **3a**. This phenomenon was also observed in **10@3a**.

Conclusions

We have described the self-assembly of two molecules of tetrakis(dihydroxyboryl)-cavitand **1a** and four molecules of 1,2-bis(3,4-dihydroxyphenyl)ethane **2** into capsule **3a** by the formation of eight dynamic boronic ester bonds in $CDCl_3$ and C_6D_6. Capsule **3a** encapsulates one guest molecule, such as 4,4′-disubstituted-biphenyl and 2,6-disubstituted-anthracene derivatives, which is oriented with the long axis of the guest directed along the long axis of **3a**, as confirmed by a ^{1}H NMR study and X-ray crystallographic analysis. Capsule **3a** strictly discriminates the functional groups of a guest, as well as a difference of one or two carbon atoms in guest size, leading to a highly selective guest recognition on encapsulation. Capsule **3a** shows a significant solvent effect on guest encapsulation. The association constant of **3a** with guests in C_6D_6 is much greater than that in $CDCl_3$ (450−48 000-fold). The encapsulation of guests within **3a** in C_6D_6 is enthalpically driven, whereas the encapsulation of guests within **3a** in $CDCl_3$ tends to be both enthalpically and entropically driven. Thermodynamic studies suggest that the small value of K_a with a considerable entropic contribution for guest@**3a** in $CDCl_3$ arises from the character of $CDCl_3$ as a guest competitor for **3a**, and not from the difference in stability of the boronic ester bonds of **3a** in both solvents. We propose a linker partial dissociation as the mechanism for guest uptake and release into and out of **3a** based on kinetic studies of guest@**3a** by 2D EXSY analysis, as well as structural analysis of guest@**3a**. The 2D EXSY studies also suggest that guest uptake in **3a** follows second-order kinetics and guest release out of **3a** follows first-order kinetics. The rotation behavior of 4,4′-diacetoxy-2,2′-disubstituted-biphenyls within **3a** was also investigated, where the elongation of 2,2′-disubstituents of guests hindered on guest rotation within **3a**.

Areas for further investigation are (1) asymmetric guest recognition of a chiral capsule[43] to be derived from **1a** and incorporating a C_2 symmetric chiral bis(catechol)-linker in place of **2** and (2) application of an asymmetric-guest@chiral-capsule to a supramolecular gyroscope directed toward unidirectional guest rotation.[37a,44]

Experimental Section

General. THF and CH_2Cl_2 were distilled from sodium-benzophenone ketyl and CaH_2, respectively, under an argon atmosphere. The other solvents and all commercially available reagents were used without any purification. ^{1}H and ^{13}C NMR spectra were recorded at 400 and 100 MHz, respectively, on a JEOL JNM-AL400 spectrometer. IR spectra were recorded on a JASCO FT/IR-460Plus spectrometer. The $CDCl_3$ and CD_2Cl_2 employed in all the ^{1}H NMR experiments were stored over K_2CO_3 prior to use, and the C_6D_6

(42) The biphenyl rotational barrier of guest **9** in $C_6D_5CD_3$ was estimated to be $\Delta G^{\ddagger} = <14.9$ kcal mol^{-1}, which was determined by the VT ^{1}H NMR.[17]

(43) (a) Yoon, J.; Cram, D. J. *J. Am. Chem. Soc.* **1997**, *119*, 11796–11806. (b) Castellano, R. K.; Nuckolls, C.; Rebek, J., Jr. *J. Am. Chem. Soc.* **1999**, *121*, 11156–11163. (c) Mateos-Timoneda, M. A.; Crego-Calama, M.; Reinhoudt, D. N. *Chem. Soc. Rev.* **2004**, *33*, 363–372. (d) Amaya, T.; Rebek, J., Jr. *J. Am. Chem. Soc.* **2004**, *126*, 6216–6217. (e) Schramm, M. P.; Rebek, J., Jr. *New J. Chem.* **2008**, *32*, 794–796.

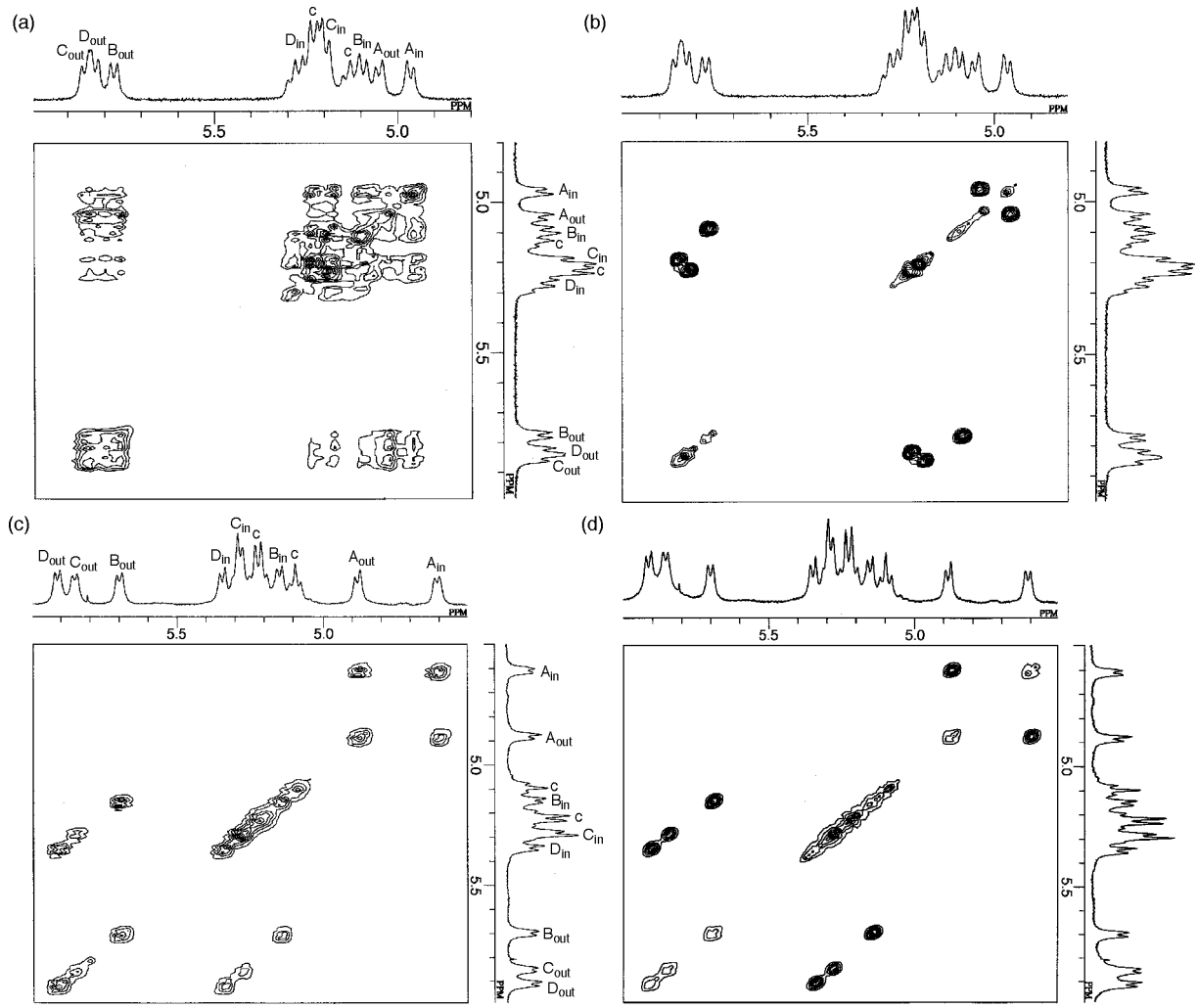

Figure 13. 2D NOESY and $^1H-^1H$ COSY spectra of **9@3a** in $C_6D_5CD_3$ (400 MHz, [**3a**] = 2.5 mM and [**9**] = 5 mM, pulse delay = 1.5 s, and mixing time = 0.5 s): (a) 2D NOESY and (b) $^1H-^1H$ COSY at 298 K; (c) 2D NOESY and (d) $^1H-^1H$ COSY at 243 K. The signals marked '$A_{in}-D_{in}$' and '$A_{out}-D_{out}$' are assigned in Figure 10. The signal marked 'c' is assigned in Scheme 1.

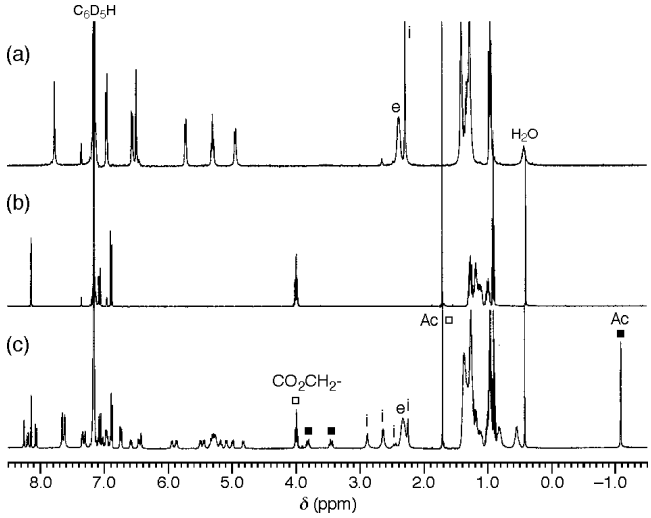

Figure 14. ^1H NMR spectra (400 MHz, C_6D_6, 298 K): (a) [**3a**] = 2.5 mM, (b) [**9**] = 5 mM, and (c) [**3a**] = 2.5 mM and [**9**] = 5 mM (**9@3a**: free-**9** = 1:1). The signals marked 'e' and 'i' are assigned in Scheme 1. The representative signals of **9** of **9@3a** and free **9** are marked with solid and open squares, respectively.

and $C_6D_5CD_3$ were stored over molecular sieves 4A prior to use. Tetrakis(dihydroxyboryl)-cavitand **1a** (R = $(CH_2)_6CH_3$), 1,2-bis(3,4-dihydroxyphenyl)ethane **2**, and guest **15** were synthesized according to the literatures.[15,45] The syntheses of other guests, X-ray data collection and crystal structure determination of **4@3b**, and 2D EXSY experiments of guest@**3a** were described in the Supporting Information.

Tetrakis(dihydroxyboryl)-Cavitand 1b (R = $(CH_2)_2$Ph). To a solution of tetrabromo-cavitand (R = $(CH_2)_2$Ph)[46] (1.00 g, 0.788 mmol) in dry THF (60 mL) at −78 °C under an argon atmosphere was added a hexane solution of *n*-BuLi (1.59 M, 2.5 mL, 4.0 mmol). After stirring for 1 h, to the resulting solution was added $B(OMe)_3$ (1.6 mL, 14 mmol) at −78 °C. The resulting mixture was stirred at −78 °C for 1 h and then allowed to warm to room temperature overnight. The reaction mixture was quenched with 2 M HCl (10 mL) at 0 °C and stirred for 30 min. After evaporation of solvents, the residue was partitioned between EtOAc (300 mL) and water (100 mL), and the organic layer was washed with water and brine and dried over Na_2SO_4. After evaporation of solvents, the residue was recrystallized from EtOAc−hexane to give **1b** as a bis-adduct of EtOAc (off-white crystals) after vacuum drying at room temperature for 12 h (617 mg, 60% yield). Mp 282 °C (decomp.);

(44) (a) Zheng, X.; Mulcahy, M. E.; Horinek, D.; Galeotti, F.; Magnera, T. F.; Michl, J. *J. Am. Chem. Soc.* **2004**, *126*, 4540–4542. (b) Horinek, D.; Michl, J. *Proc. Natl. Acad. Sci. U.S.A.* **2005**, *102*, 14175–14180.
(45) Orita, A.; Taniguchi, H.; Otera, J. *Chem.—Asian J.* **2006**, *1*, 430–437.
(46) Sherman, J. C.; Knobler, C. B.; Cram, D. J. *J. Am. Chem. Soc.* **1991**, *113*, 2194–2204.

^{1}H NMR (DMSO-d_6) δ 8.08 (s, 8H), 7.53 (s, 4H), 7.16−7.25 (m, 20H), 5.53 (d, J = 7.8 Hz, 4H), 4.63 (t, J = 7.3 Hz, 4H), 4.43 (d, J = 7.8 Hz, 4H), 3.30−3.33 (m, 8H), 2.53−2.62 (m, 8H); ^{13}C NMR (DMSO-d_6) δ 155.5, 141.8, 137.2, 128.6, 128.4, 128.3, 125.8, 121.5, 98.7, 36.5, 34.2, 31.9. Anal. Calcd for $C_{64}H_{60}B_4O_{16}$·2(EtOAc): C, 66.29; H, 5.87. Found: C, 66.08; H, 6.15.

Capsule 3a. A suspension mixture of **1a**·OEt_2 (50.00 mg, 42.4 mmol) and **2** (20.89 mg, 84.8 mmol, 2 equiv) in $CDCl_3$ (or $CHCl_3$) (8.5 mL) was stirred at 50 °C for 3 h. The ^{1}H NMR spectrum of the resulting homogeneous solution showed the quantitative formation of **3a** (see Figure 1c). After evaporation of solvents, the residue was dried in vacuo at room temperature for 5 h. The dried sample of **3a** was initially less soluble in $CDCl_3$ at room temperature, but after heating in $CDCl_3$ at 50 °C for several minutes, **3a** became soluble again at room temperature. Heating a 2:4 mixture of **1**·OEt_2 and **2** in C_6D_6 (or C_6H_6) at 50 °C for 3 h with stirring did not give a homogeneous system, although **3a** was quantitatively formed (Figure 1f). The solubility of **3a** in C_6D_6 at 23 °C was 1.3 mM based on the ^{1}H NMR integration ratio with *p*-dimethoxybenzene as an internal standard. ^{1}H NMR ($CDCl_3$, 296 K, 2.5 mM) δ 7.37 (s, 8H), 7.27 (d, J = 7.8 Hz, 8H), 7.11 (d, J = 1.9 Hz, 8H), 7.06 (dd, J = 1.9 and 7.8 Hz, 8H), 5.67 (d, J = 7.3 Hz, 8H), 4.89 (t, J = 8.3 Hz, 8H), 4.63 (d, J = 7.3 Hz, 8H), 2.97(s, 16H), 2.27−2.37 (m, 16H), 1.25−1.53 (m, 80H), 0.93 (t, J = 6.3 Hz, 24H); ^{1}H NMR (C_6D_6, 296 K, 1.3 mM) δ 7.77 (s, 8H), 6.95 (d, J = 7.8 Hz, 8H), 6.55 (d, J = 7.8 Hz, 8H), 6.49 (s, 8H), 5.72 (d, J = 6.8 Hz, 8H), 5.29 (t, J = 7.8 Hz, 8H), 4.93 (d, J = 6.8 Hz, 8H), 2.34−2.42 (m, 16H), 2.28 (s, 16H), 1.20−1.44 (m, 80H), 0.95 (t, J = 6.8 Hz, 24H).

Guest@3a. To as-prepared **3a** in an NMR tube was added a stock solution of a guest in $CDCl_3$ or C_6D_6. The resulting mixture was heated at 50 °C for 30 min to give a solution of guest@**3a**.[17] Alternatively, to a 2:4 mixture of **1a**·OEt_2 and **2** in an NMR tube was added a stock solution of a guest in $CDCl_3$ or C_6D_6, and the resulting mixture was heated at 50 °C for 3 h to give a solution of guest@**3a**. A solution of **8**@**3a** in C_6D_6 was prepared at 0.5 mM because of its solubility problem. In all other cases, a solution of guest@**3a** or a mixture of guest@**3a** and free **3a** were prepared at 2.5 mM in total.

Acknowledgment. We thank Prof. A. Orita (Okayama University of Science) for the gift of guest **15**. We also thank Prof. T. Haino (Hiroshima University) for valuable discussions. This work was supported in part by PRESTO, JST.

Supporting Information Available: Additional data and X-ray crystallographic data (CIF). This material is available free of charge via the Internet at http://pubs.acs.org.

JA9084918